An Absorbed Dose to Water Primary Standard for Ir-192 Brachytherapy

by

Islam Mohamed Medhat El Gamal

A thesis submitted to the Faculty of Graduate and Postdoctoral Affairs in partial fulfillment of the requirements for the degree of

Master of Science

in

Physics

Ottawa-Carleton Institute for Physics
Department of Physics
Carleton University
Ottawa, Ontario

Abstract

The goal of this work was to develop an absorbed dose to water primary standard for Ir-192 brachytherapy by using a Fricke dosimeter. The radiation chemical yield (G-value) of the Ferric ions in the Fricke solution was measured at Co-60 and 250 kVp X-ray, yielding 1.610 ± 0.010 μmol J^{-1} and 1.602 ± 0.009 μmol J^{-1} respectively. A log-linear interpolation was conducted based on the two standard beam values to realize the radiation chemical yield at Ir-192 energy of 1.605 ± 0.005 μmol J^{-1}. A PMMA holder was developed for irradiations using an Ir-192 brachytherapy source and a final uncertainty on the dose to water at the reference position of 0.7 % was achieved, in agreement with NRC air-kerma based standards at the 2σ level. The largest contributing factor to this uncertainty was the G-value at 250 kVp X-ray. A reduction in the G-value uncertainty gives the system the potential to provide an even lower uncertainty on the absorbed dose to water at the reference position.

Acknowledgements

I would like to thank my supervisor Dr. Malcolm McEwen, Dr. Carl Ross and Dr. Claudiu Cojocaru for their help, guidance, patience and support without which this work would not have been possible.

Also, I would like to thank Brad Downton and Hong Shen for making time and helping out with the irradiations throughout this work. David Marchington for building the holders and countless other devices used throughout this work. Dr. Ernesto Mainegra-Hing for painstakingly modeling all the experimental setups and doing all the Monte Carlo simulations and Dr. Paul Johns for his patience, encouragement and support.

I would also like to thank everybody at the ionizing radiation standards group for always being there to help and for making my time at NRC an unforgettable one. I would like to thank Dr. Addass, Dr. Omar and Dr. Samman for pushing me to pursue graduate studies.

Finally, I would like to thank my family and friends for their support and encouragement over the past two years.

Table of Contents

List of Tables

List of Figures

List of Appendices

1 Chapter: Introduction

1.1 Brachytherapy

Brachytherapy is a radiation therapy treatment modality that involves placing a radioactive source within or close to the tumor volume. It provides a therapeutic gain over conventional external beam radiotherapy, EBRT, by lowering the dose delivered to normal tissue. The reduction in normal tissue dose can be attributed to the radiation not having to travel through normal tissue to reach the treatment site as opposed to EBRT.

Brachytherapy can be classified as low dose rate, LDR, and high dose rate, HDR, depending on the source used. LDR sources such as Iodine-125 or Palladium-103 are usually implanted surgically into the treatment volume, the procedure is less invasive than surgery but involves dose to clinical staff and issues regarding source migration within the patient. HDR sources such as Iridium-192 are delivered for a predetermined amount of time to the treatment volume, via a catheter, using an after-loader. HDR-brachytherapy is often used as a boost with EBRT and an adequate fractionation regime can allow it to replace some LDR implants.

The development of after-loading technology has increased the number of patients receiving brachytherapy. After-loaders store the radioactive sources, also called seeds, in a shielded compartment that reduces the dose to background levels. A catheter is placed in the treatment volume and connected to the after-loader. When the treatment begins the

after-loader is operated from outside the bunker and the seed is pushed through the catheter at the end of a steel cable. The after-loader is calibrated to deliver the seed at a fixed position within the catheter and can be programmed to withdraw the seed after a preset time. The use of after-loaders has virtually eliminated the dose to clinical staff providing HDR-brachytherapy. The HDR Ir-192 brachytherapy seeds investigated in this work are chiefly applied to the treatment volume using after loader technology allowing the dose delivered to be controlled by varying the time the seed is allowed to remain within the volume, known as the dwell time. Ir-192 is produced through the neutron activation of naturally abundant Ir-191. The resulting isotope has a complex spectrum with average decay energy of 0.38 MeV. Ir-192 has a half-life of 73.810 ± 0.019 d and sources typically have a specific activity of 9.22×10^3 Ci/g (Delacroix et al, 1998).

1.2 Brachytherapy Dosimetry

The absorbed dose is defined as the energy deposited in a medium per unit mass at the point of measurement, and is the primary measure of the biological effects of ionizing radiation. The goal of any reference dosimetry protocol is the determination of the absorbed dose to the patient. However, the practical goal is to determine the absorbed dose to water, D_w. This is typically achieved using a primary standard, a device that gives the lowest possible uncertainty on the quantity of interest. The primary standard is then used to calibrate clinical instruments. To date the American Association of Physicists in Medicine, AAPM, task group 43, report (1995) along with its update (2004) forms the

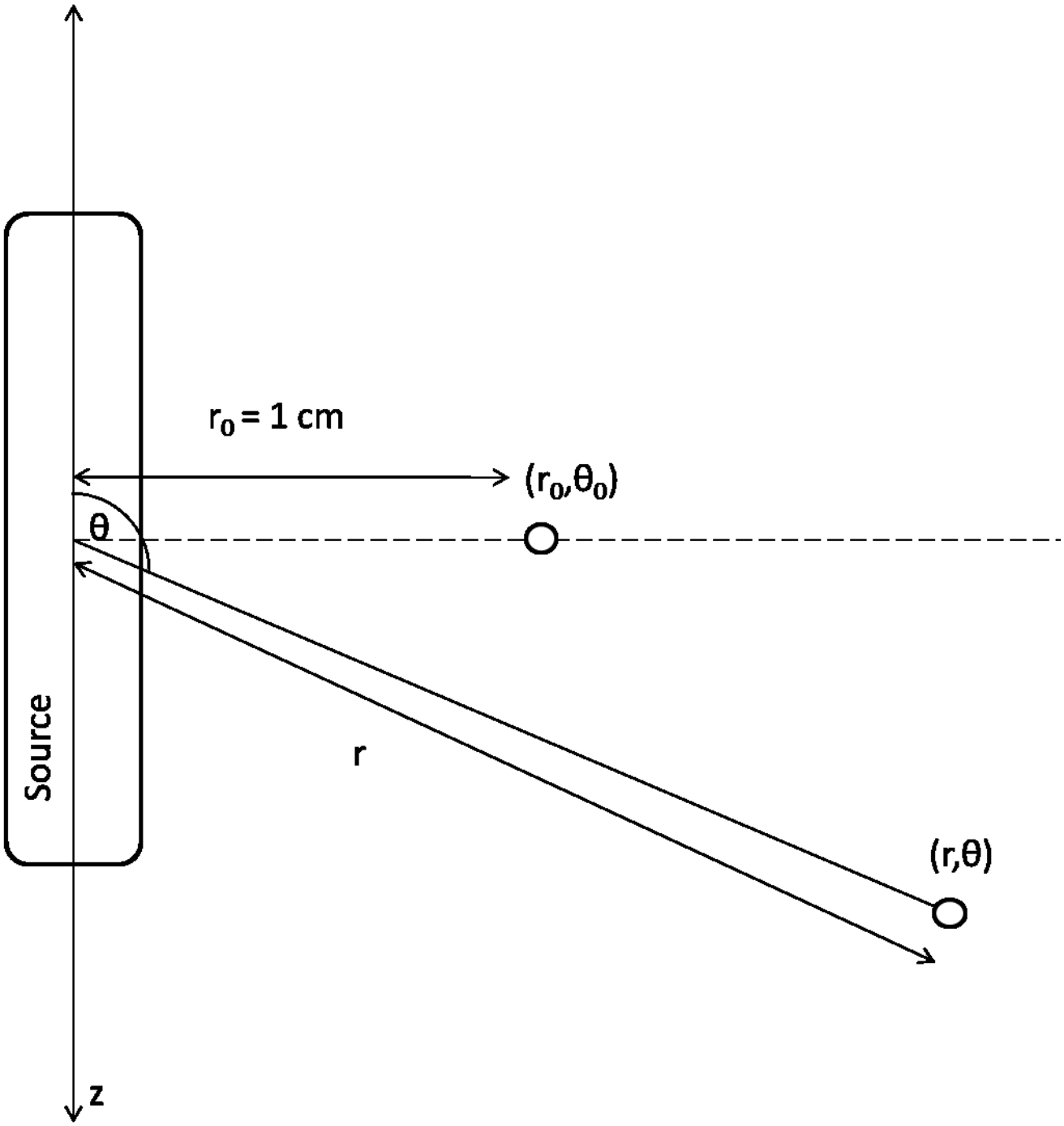

Figure 1 Coordinate system used by the TG-43 dosimetry protocol

basis of brachytherapy dosimetry in North America. The TG-43 formalism employs the polar coordinate system used in figure 1, where r denotes the transverse distance from the longest side of the source whilst θ denotes the polar angle. The dose rate at a point (r,θ) is thus defined for a point source by:

$$\dot{D}(r,\theta) = \dot{D}(r_0,\theta_0)\left(\frac{r_0}{r}\right)^2 [g_p(r)\,\varphi_{an}(r)], \qquad (1.1)$$

where,

$\dot{D}(r_0,\theta_0)$ denotes the dose rate at the reference position taken by convention to be at r=1cm and θ=90°,

$g_p(r)$ is the radial dose function using the point source approximation and represents the relative decrease in dose along r due to the attenuation and scattering of photons by water,

$\varphi_{an}(r)$ is the 1-D anisotropy function defined for a given *r* as $\frac{\int_0^{\pi}\dot{D}(r_0,\theta)\sin\theta\,d\theta}{2\dot{D}(r,\theta_0)}$, which represents the dose rate, solid angle weighted, averaged over 4 π space divided by the dose rate at the same point on the transverse $\theta = \theta_0$ plane.

Only the point source approximation is mentioned for simplicity. It should be noted that the quantities in square brackets in equation 1.1, as used clinically, are not measured but calculated numerically. The dose rate at the reference position, the quantity to be determined by a metrology primary standard, is defined in TG-43 as:

$$\dot{D}(r_0,\theta_0) = S_k\,\Lambda, \qquad (1.2)$$

where,

S_K is the air-kerma strength with units of cGy cm^2 h^{-1}, denoted by U, and

Λ is the dose rate constant with units of cGy $h^{-1}U^{-1}$

Air-kerma strength is further defined as:

$$S_k = [\dot{K}_\gamma\,(d)]d^2, \tag{1.3}$$

where $K_\gamma\dot{(d)}$ denotes the air-kerma rate in vacuo, the rate of kinetic energy transfer by photons to electrons at the point of photon interaction per unit mass of air, and *d* the distance from the source center to the point at which the air-kerma rate is measured. The distance *d* is chosen such that it is large compared to the source and detector dimensions, usually taken to be on the order of 1 meter, making S_K independent of *d*. S_K at Ir-192 energy is conventionally determined by taking 7 in air measurements at different calibration distances using a secondary standard ion chamber (Goetsch et al, 1991). The ion chamber's air-kerma calibration coefficients are determined by interpolating using a weighted average the chambers calibration coefficients at Cs-137 and 250 kVp x-ray energies (DeWerd et al, 2011).

Since the air-kerma rate in vacuo is the desired quantity, the measured value has to be corrected for any attenuating effects of air and photon scattering. γ in equation 1.3 is intended to be an energy cut-off value to exclude the contributions to the air-kerma strength from low energy contaminant photons which only contribute to the dose at distances of less than 0.1 cm in tissue. The importance of an energy cut-off is greatest for low energy photon sources and is typically on the order of 5 keV (Rivard et al, 2004).

Using the 7 distance method described above, uncertainties on S_K on the order of 3 % are typical on end user well chambers (Stump et al, 2001). More recently a comparison between well chambers calibrated at the National Institute of Standards and Technology, NIST, and the National Physics Laboratory, NPL, showed a 2.6 % difference in the dose rates measured for the same source (Rasmussen et al, 2011).

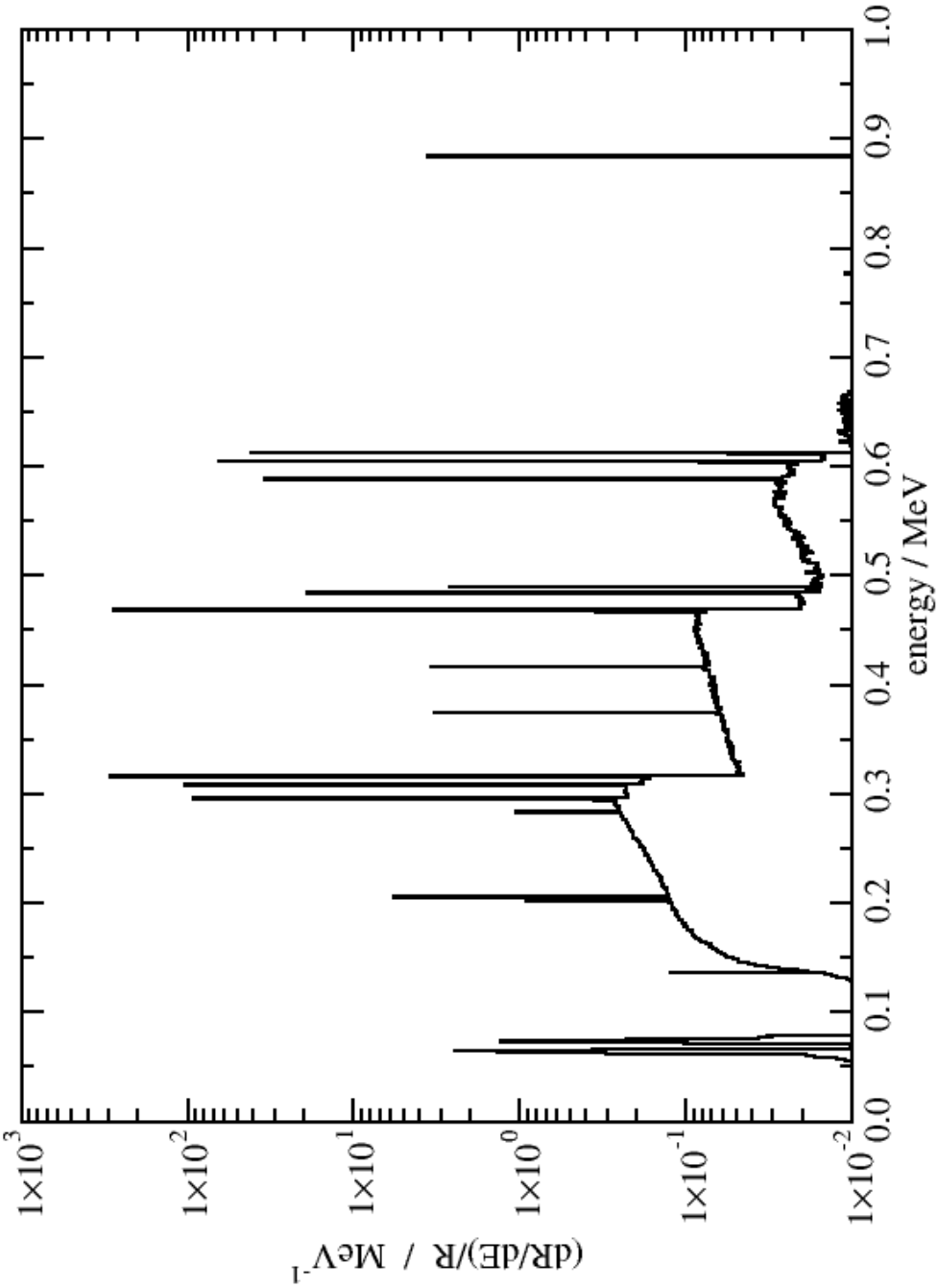

Figure 2 Ir-192 Photon spectrum (CLRP, 2008)

where, R denotes the total energy of photons escaping the source encapsulation and E the photon energy.

The dose rate constant, as defined in equation 1.2, depends on the type of radionuclide, the source encapsulation design and composition. Unlike some low energy sources such as I-125 where the dose rate constant is determined as an average of Monte Carlo and experimental values, at Ir-192 energies the present determination is entirely Monte Carlo based. The reliance on Monte Carlo is attributed to conventional detector radio-sensitivity, energy response, positioning uncertainties and volume averaging effects (Perez-Calatayud et al, 2012). The importance of the dose rate constant should be highlighted as it converts the relative TG-43 dose rate distribution into an absolute one.

1.3 Dosimetric Alternatives

Reliance on an air-kerma based standard can be attributed to the difficulties associated with near field dosimetry. The high dose gradients surrounding a brachytherapy seed require a detector with a small active volume and high resolution to provide an acceptable dose non-uniformity correction (Chiu-Tsao et al, 2007). Estimates on the dosimetric uncertainties of D_w for some conventional air-kerma independent methods were summarized by DeWerd et al (2011) for high energy brachytherapy photon sources, > 50 keV:

- Radiochromic Film 10 %
- Diamond diode and other solid state detectors > 15 %
- Thermoluminescent LiF Dosimeters > 6 %

Research into calorimeter based Ir-192 brachytherapy dosimetry by Sarfehnia et al (2007) has been able to overcome the challenges associated with source self-heating, heat loss and positioning uncertainty. The parallel plate calorimeter developed has the potential for a combined D_w uncertainty of less than 5 %, with similar results being achieved in European standards labs using graphite calorimeters (Selbach, 2012) and is thus far the most promising air-kerma independent method for the determination of D_w.

1.4 Basis of project

By developing an air-kerma independent system to determine D_w at the reference position directly the same TG-43 formalism may be maintained with a reduced uncertainty on D_w. This will in part be due to not having to rely on a Monte Carlo determination of the dose rate constant which has been shown to be sensitive to voxel size effects, reaction cross sections and source design (Taylor, 2008).

Ideally, as recommended by the TG-43 update (2004), a detector should:

- Have a small active volume
- Well characterized energy response
- Sufficient precision such that at 1σ type A uncertainty should be less than 5% and type B uncertainty should be less than 7% on D_w

This work shows that a Fricke based dosimeter satisfies all these requirements allowing for an air-kerma independent method for the determination of D_w for an HDR Ir-192 brachytherapy source with a target standard uncertainty below 1.5 % (k=1). In chapter 2 an introduction to Fricke dosimetry is provided whilst chapters 3 and 4 outline the determination of the radiation chemical yield of Ferric ions and the development of the

dosimeter respectively. Chapters 4 and 5 show the calculated dose to water at the reference position and give an overview of the conclusions reached by the project. All of the experiments, results and analysis present in this work were conducted by the author except for the radiation transport calculations which were performed by Dr. Ernesto Mainegra-Hing of the Canadian ionizing radiation standards laboratory.

2 Chapter: Fricke Dosimetry

2.1 Introduction

Fricke dosimetry is a chemical dosimetry system developed by Hugo Fricke (Fricke and Hart, 1966). Being closely water equivalent and having a high sensitivity in the dose range of interest in radiotherapy has made it the most widely used chemical dosimeter. The main constituents of the dilute aqueous Fricke solution are sulphuric acid and ferrous ammonium sulfate. The dosimeter relies on measuring the ferric ions (Fe^{3+}) produced through the oxidation of ferrous ions (Fe^{2+}) in the solution by water radiolysis products. The yield of ferric ions can consequently be related to the dose imparted to the Fricke solution.

2.1.1 Fricke solution preparation

The following procedure was used to make Fricke solution in this project following the work of Olszanski et al (2002):

- A 2 L quartz flask is rinsed 5 times with Millipore water (ultra-pure water with less than five parts per billion, < 5 ppb, of impurities)
- The flask is filled with 1500 g of Millipore water
- A beaker is rinsed 5 times with the acid to be used
- The mass of sulphuric acid to be added (JT Baker and Company, Philipsburg, Ultrex 2 grade 95.5% acid was used) to the beaker is determined using:

$$Mass\ of\ acid\ (g) = \frac{0.4\ (M) \times 2(L) \times 98.08\ (g\ mol^{-1}) \times 100}{\%\ acid\ concentration} \quad (2.1)$$

- The acid is dispensed from the beaker to the 2 L quartz flask
- A Co-60 unit is used to pre-irradiate the water acid mixture to 10 Gy, in order to remove a non-linearity of solution response at low doses due to trace impurities
- 0.784 g of ferrous ammonium sulfate, 99.997% purity, is added to the flask
- 0.1169 g of sodium chloride, 100% purity, is added to the flask
- Millipore water is added until the solution reaches a mass of 2043.4 g to ensure the correct concentration of reactants is achieved
- The solution is air saturated by swirling it around within the flask while periodically removing the stopper
- Once air saturated the solution is covered and kept away from all sources of light, to avoid any light induced reactions in the solution

It should be noted that there are several variations in the literature to the NRC method of producing Fricke solution, primarily in the acid concentration and the use of NaCl.

2.2 Reaction mechanism

Once the Fricke solution is irradiated, a number of reactions (at least 50 are known), take place. The highest yield and hence the most relevant reactions are shown (Jayson et al, 1975,Klassen et al, 1999,McEwen and Ross, 2009):

$$H\cdot + O_2 \rightarrow HO_2\cdot \quad (2.2)$$

$$HO_2\cdot + Fe^{2+} \rightarrow HO_2^{-} + Fe^{3+} \quad (2.3)$$

$$HO_2^{-} + H^{+} \rightarrow H_2O_2 \quad (2.4)$$

$$H_2O_2 + Fe^{2+} \rightarrow HO^{-} + Fe^{3+} + HO\cdot \quad (2.5)$$

$$HO\cdot + Fe^{2+} \rightarrow HO^{-} + Fe^{3+} \quad (2.6)$$

$$H\cdot + H_2O \rightarrow HO\cdot + H_2 \quad (2.7)$$

These reactions highlight two important features of the Fricke dosimeter: that the oxidation of ferrous ions is due to reactions involving the radiolysis products of water and that the Ferric ion yield is oxygen dependent, hence the need to air saturate the solution. The oxygen dependence is due to reaction 2.2 being replaced by reaction 2.7 in the absence of oxygen thus reducing the ferric ion yield. The slowest reaction, 2.5**,** has a half-life of 14 s meaning that the reactions are expected to come to completion before the readout procedure can begin (McEwen and Ross, 2009). The ferric ion yield is believed to be stable over the course of several days as demonstrated by the use of Fricke solution as a mail audit dosimeter in other investigations (McEwen and Ross, 2009).

2.3 Readout procedure

In order for the Fricke solution to be useful as a dosimeter, the yield of Ferric ions must be easily determined. In the past titrimetry was used to determine the ferric ion yield but the relative speed and automation of modern spectrophotometers has made them the preferred choice. The creation of ferric ions produces a measurable change in the optical absorbance of the Fricke solution which may be measured using a spectrophotometer. Figure 3 shows the absorption spectrum of ferric ions. There are two broad peaks centered at 303 and 224 nm which can be used to measure the change in the optical absorption of the Fricke solution. Although the 224 nm peak provides a larger signal for measurement, the 303 nm peak was used throughout this work. The use of 303 nm is attributed to large variations in the readout signal at 224 nm believed to be due to the presence of contaminants or the products of chemical reactions involving contaminants. When irradiations are conducted in non-glass vials it appears that the contaminants have a peak close to 224 nm hence explaining the large variations only observed at 224 nm. The optical density is the quantity being measured and is defined as:

$$OD = log_{10}\left(\frac{I_0}{I}\right) \ , \tag{2.8}$$

where I_0 and I denote the incident and transmitted beam intensities respectively. The absolute value of I_0 is not important since all optical density values used to determine dose are calculated as the difference of two optical density readings with the same I_0.

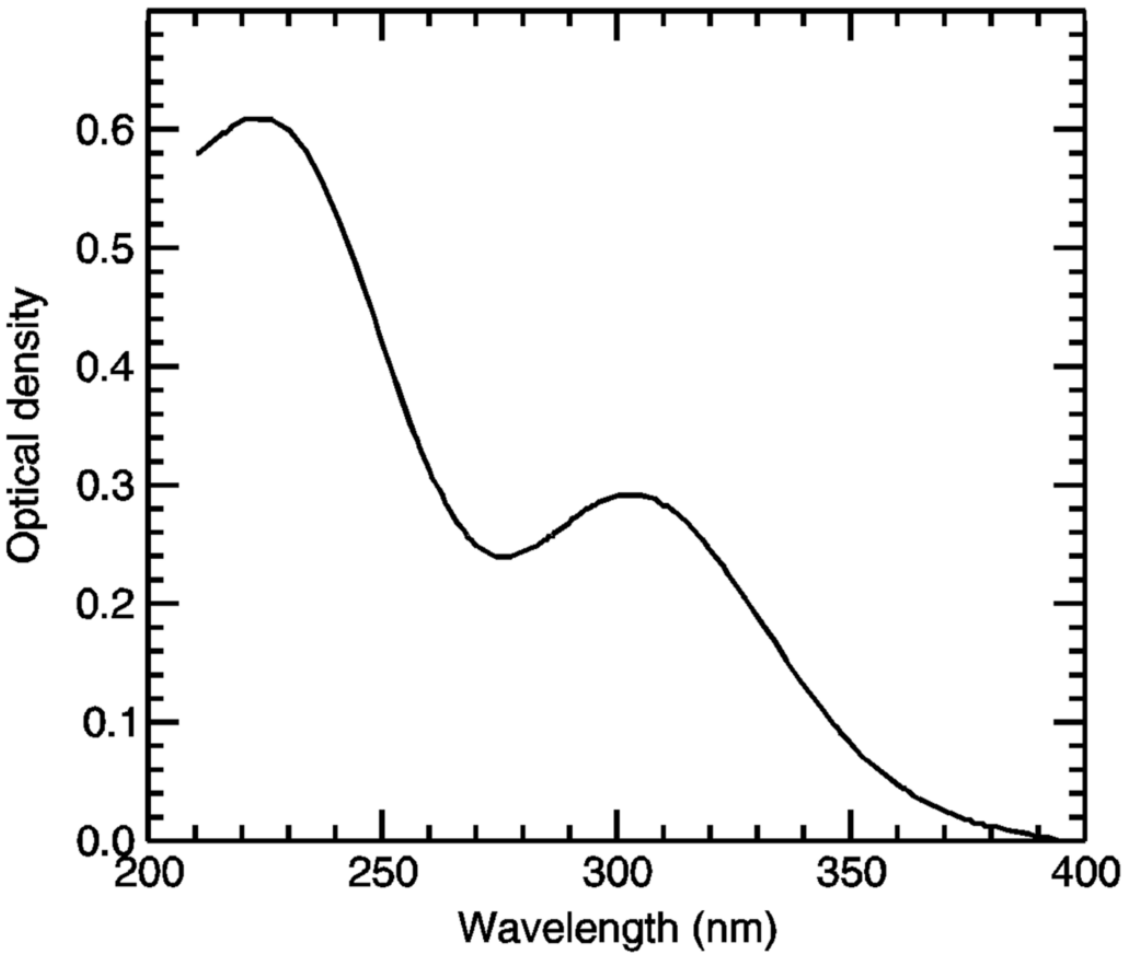

Figure 3 Fe^{3+} ion absorption spectrum (McEwen and Ross, 2009)

The following readout procedure was used to determine the change in the optical density of the Fricke solution:

- All relevant surfaces are cleaned using Millipore water
- Tap on Fricke funnel is opened for approximately 2 minutes, to dispose of Fricke solution at the bottom of the funnel that has been exposed to light
- Plastic tweezers rinsed 5 times with Millipore water
- Glass dishes are rinsed 5 times with Millipore water
- 1 mm path length quartz cuvettes ,Figure 4, are removed from Millipore water filled beaker using plastic tweezers and placed in glass dishes
- 3 beakers are rinsed 5 times with Millipore and then filled with Millipore water
- A beaker is rinsed 5 times with sulphuric acid (JT Baker and Company, Philipsburg, Ultrex 2 grade 95.5%) and then filled with sulphuric acid
- The aspirator is cleaned with the acid and then rinsed 20 times in each Millipore water filled beaker
- The cuvettes are rinsed and dried twice using Millipore water with the aspirator being rinsed 20 times in each Millipore water filled beaker between cuvette rinses
- A cotton Q-tip applicator is rinsed with Millipore water then used to clean the inside of the cuvette first then the outside transparent windows
- The cuvette windows are rinsed 10 times with Millipore water and dried using compressed nitrogen gas
- The cuvettes are rinsed and dried 3 times using Millipore water and the aspirator
- The cuvettes are rinsed using the Fricke solution to be measured, where the solution is transferred using a pipette (see Appendix A.1) but not dried before the

remainder of the solution is inserted such that the surface of the solution is at least 1.7 mm above the bottom

- The cuvette Teflon lid is rinsed with Millipore water and dried using compressed nitrogen gas
- The sealed cuvette is placed in a modified Cary 400 (Varian, Palo Alto) spectrophotometer for readout at 303 nm

The detail given is necessary for the results to be reproducible and highlights the sensitivity of the Fricke, or any, chemical metrology system, to contamination. Contamination affects the optical density directly or results in the production of chemical species that affect the optical density readings. The modified Cary 400 spectrophotometer (Olszanski et al, 2002) keeps the sample compartment, Figure 5, containing the cuvettes at 25.00 ± 0.01 °C and uses compressed nitrogen purging to limit contamination of the spectrophotometer's optics. A custom program allows the readout process to be automated. During readout the sample compartment can hold two cuvettes, an empty sample compartment and a standard absorbance filter. A 30 % transmittance NIST SRM-2031 metal-on-quartz standard absorbance filter is used with an expected absorbance reading at 303 nm of 0.355 optical density units. The role of the filter is to verify that the reliability of the absorbance readings given the effects of zero drift or misalignment of the sample compartment with the optical components of the spectrophotometer.

The program takes absorbance readings four times for each sample, twice for the filter and once for the empty slot before each sample measurement. The empty slot is measured to verify the zero or background absorbance reading to be subtracted from the next sample measurement. All absorbance readings are taken using the double beam mode

with the reference beam passing through air. Each absorbance reading is in fact the average of 5 individual readings made over 2 seconds with an additional 2 seconds waiting time between readings. The program allows 5 minutes before measurements can begin in order for thermal equilibrium to occur between the cuvettes and the sample compartment. Figure 6 shows a sample readout report for an irradiated Fricke solution.

The reproducibility of the optical density readings, to within 0.2 % over 8 years when irradiated using a cobalt 60 unit (Klassen et al, 1999), demonstrates the system's potential for use in high precision applications.

To determine the net, radiation induced, change in optical density readings a set of controls have to be measured each day and subtracted from the irradiated optical density readings. A control measurement is needed to account for contamination effects of irradiating the Fricke in non-glass holders and to account for the observed increased optical density of un-irradiated Fricke solution, 0.0004 optical density units per day at 303 nm (Klassen et al, 1999, Olszanski et al, 2002), due to storage effects. Throughout this work a Fricke control refers to a measurement whereby the Fricke solution undergoes the same procedure for irradiation, i.e. being transferred to an irradiation vessel, placed in a phantom etc… , without being irradiated.

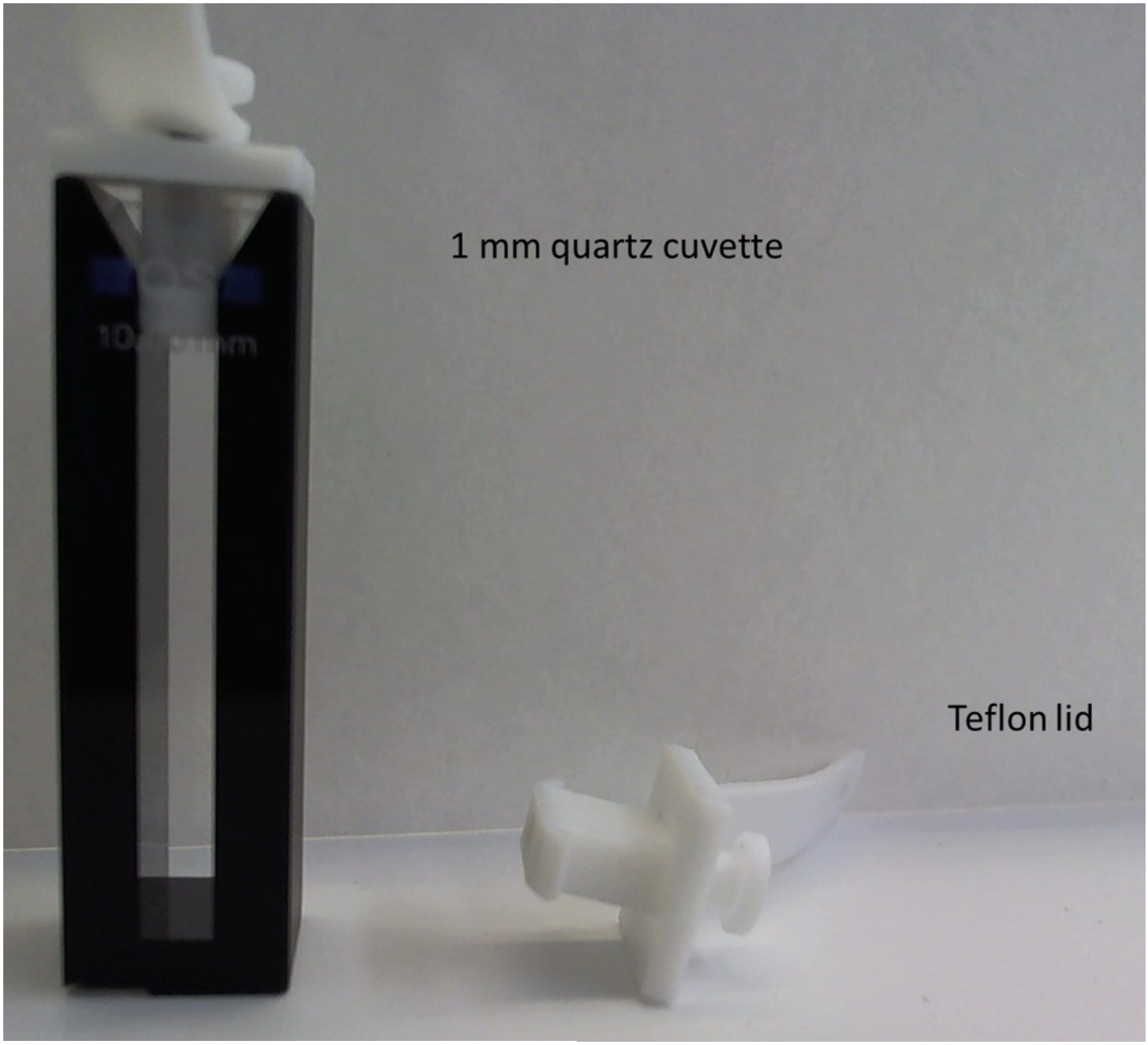

Figure 4 Quartz cuvette and Teflon lid

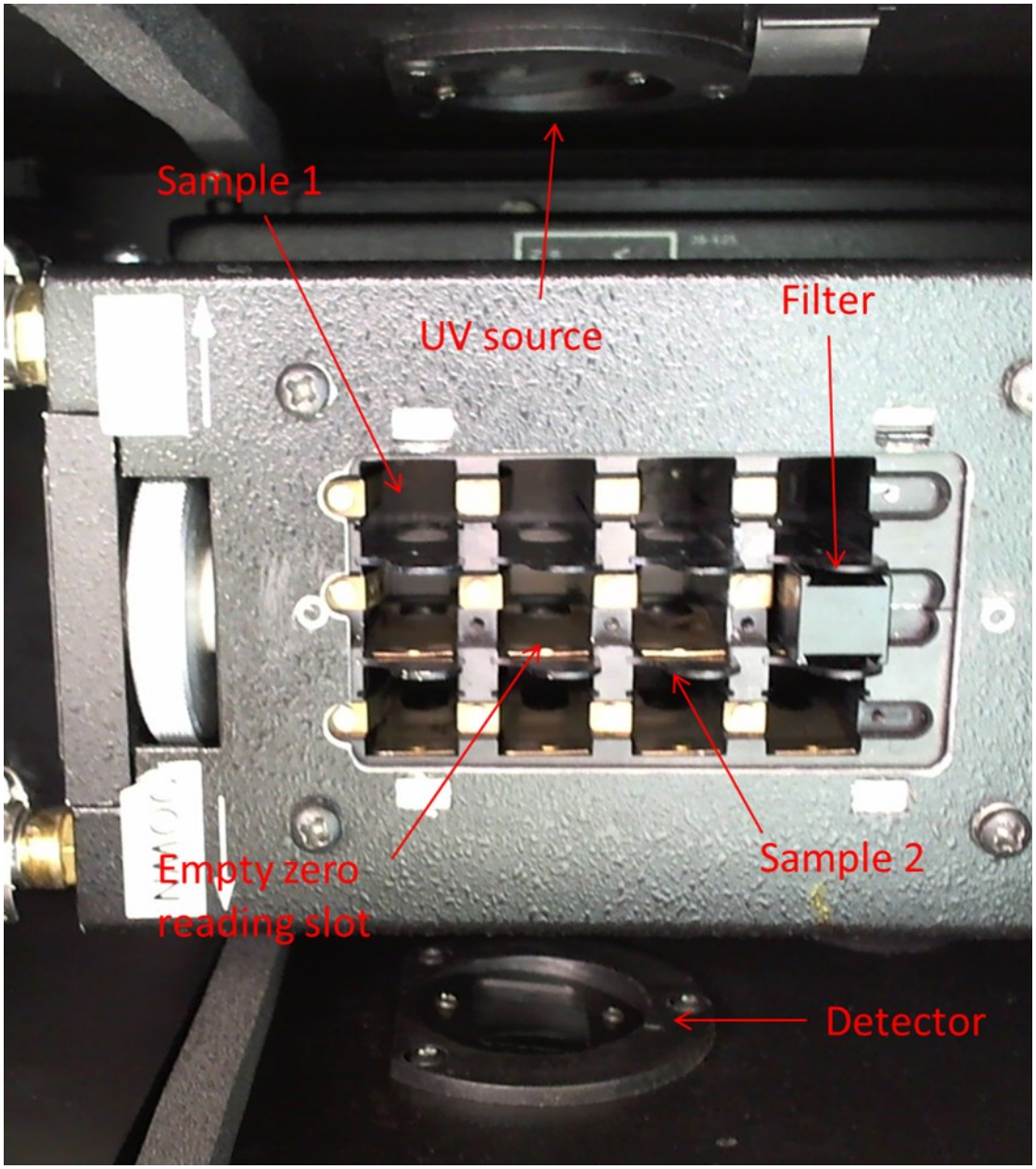

Figure 5 Cary 400 modified sample compartment

2.4 Dose to Fricke determination

Once the change in optical density is determined the dose to the Fricke solution can be obtained from:

$$D_F = \frac{\Delta OD_{net}}{\varepsilon \cdot G(Fe^{3+}) \cdot \rho \cdot d}, \quad (2.9)$$

The net change in optical density is denoted by ΔOD_{net} . In order to determine the dose, this quantity has to be divided by the product of ρ the Fricke solution density, taken to be 1.0227 x 10^{-3} kg cm^{-3} at 25 °C (Olszanski et al, 2002), and *d* the optical path-length of the cuvette used for readout. The optical path length of a cuvette is defined as the product of the distance traversed by light through the cuvette and the refractive index of the cuvette window. For this work 1 ± 0.0002 cm (Klassen et al, 1999) optical path length cuvettes were used.

The molar linear absorption coefficient, denoted by ε, quantifies the effect of one mole of ferric ions on the optical density reading and is similar to an attenuation coefficient for x-rays traversing a material. The molar linear absorption coefficient is a constant chemical property of the ferric ions and has been measured at 25 °C to be 2174 x 10^3 cm^2 mol^{-1}. The radiation chemical yield of the ferric ions, (Fe^{3+}) , or G-value represents the number of moles of ferric ions produced per joule of energy deposited in the Fricke solution. At this point the temperature dependence of the optical density should be highlighted. Since both the density and molar linear absorption coefficient are defined by convention at 25 °C the optical density reading should consequently be determined when the solution is

irradiated at 25 °C and read out in the spectrophotometer at 25 °C. It has been shown that the G-value at a given beam quality decreases by 0.12 % per °C decrease in irradiation temperature, T_{irrad}, and the molar linear absorption coefficient shows a 0.69% decrease per °C decrease in readout temperature, T_{read},(Klassen et al, 1999, Shortt, 1989) . To account for this the following relationship is used to convert the optical density readings at an arbitrary irradiation temperature and readout temperature to one at the reference temperature of 25 °C (Klassen et al,1999):

$$\Delta OD_{25,25} = \Delta OD_{T_{irrad},T_{read}} \cdot [1 + 0.0012(25 - T_{irrad})][1 + 0.0069(25 - T_{read})] , \quad (2.10)$$

2.5 G-value variation

A discussion of the variation of the G-value with beam quality helps yield an insight into the interaction of radiation with the Fricke solution. Based on reactions 2.2–2.7 the G-value may be expressed as the sum of the individual chemical yields of the water radiolysis products responsible for the oxidation of the ferrous ions (La Verne and Schuler, 1994):

$$G(Fe^{3+}) = 2G(H_2O_2) + 3G(H) + G(OH) , \quad (2.11)$$

Figure 7 shows a semi-log plot of historical G-value results versus equivalent photon energy, collected by Klassen et al (1999). There is a clear decrease of G-value with decreasing equivalent photon energy whilst at higher energies the G-value seems to be

Figure 6 Sample spectrophotometer report

Date:10-06-2013 Run #1

#	Slot#	SampleID	Vial#	Wavelength	T(irrad)	T(read)	Absorbance	NetAbsorbance
1	2	Zero	N/A	303 nm	N/A	24.99°C	0.000027	0.000000
2	1	Sample1	1	303 nm	25.00°C	25.00°C	0.315903	0.315876
3	2	Zero	N/A	303 nm	N/A	24.99°C	0.000065	0.000000
4	3	Sample2	3	303 nm	25.00°C	24.99°C	0.047816	0.047752
5	4	Filter	N/A	303 nm	N/A	25.00°C	0.355370	0.355305
6	3	Sample2	3	303 nm	25.00°C	24.99°C	0.047601	0.047536
7	2	Zero	N/A	303 nm	N/A	24.99°C	-0.000103	0.000000
8	1	Sample1	1	303 nm	25.00°C	24.99°C	0.315914	0.316017
9	2	Zero	N/A	303 nm	N/A	24.99°C	0.000006	0.000000
10	1	Sample1	1	303 nm	25.00°C	24.99°C	0.315959	0.315953
11	2	Zero	N/A	303 nm	N/A	24.99°C	0.000031	0.000000
12	3	Sample2	3	303 nm	25.00°C	24.99°C	0.047817	0.047786
13	4	Filter	N/A	303 nm	N/A	24.99°C	0.355213	0.355182
14	3	Sample2	3	303 nm	25.00°C	25.00°C	0.047720	0.047689
15	2	Zero	N/A	303 nm	N/A	24.99°C	-0.000132	0.000000
16	1	Sample1	1	303 nm	25.00°C	24.99°C	0.315909	0.316042

RESULT:

Slot#	SampleID	SampleType	Vial#	Cuvette#	Wavelength	T(irrad)	T(Read)	Absorbance
->1	Sample1	Irrad.	1	X	303 nm	25.00°C	24.99°C	0.31597
->2	Zero	None	N/A	None	303 nm	N/A	24.99°C	0.00000
->3	Sample2	Irrad.	3	XII	303 nm	25.00°C	24.99°C	0.04769
->4	Filter	Filter2	N/A	None	303 nm	N/A	24.99°C	0.35524

Net absorbance = Absorbance – most recent zero reading

Averaged Net absorbance readings

Average Sample **compartment temperature**

relatively independent of beam quality. The relation can be explained in general terms if one considers that when the Fricke solution is irradiated three dominant interactions occur involving water radiolysis products: intra-track reactions, diffusion and scavenging (Pimblott and La Verne, 2002).

Intra-track reactions involve radiolysis products produced along the same ionizing radiation track reacting with one another and recombining without oxidizing ferrous ions thus reducing the G-value. Diffusion of radiolysis products allows the oxidation of ferrous ions to occur thus increasing the G-value, whilst scavenging involves the interaction of the water radiolysis products with impurities, primarily organic impurities, without oxidizing the ferrous ions thus reducing the G-value, although possibly increasing the optical density reading due to the formation of new chemical species. Based on these reaction mechanisms alone the apparent decrease in G-value with decreasing equivalent photon energy or equivalently, increasing linear energy transfer, LET, can be attributed to increased intra-track interactions due to the more densely ionizing high LET radiation.

For completeness it should be noted that for very high LET radiation, > 2000 MeV/cm, such as heavy ions, LET is a poor specifier of the expected G-value (Axtman and Licari, 1964). At such high values of LET the effects of track structure dominate and consequently the ratio of the square of the ionizing particles charge to the square of its velocity proves to be a more adequate specifier (Pimblott and La Verne, 2002). Since this work only

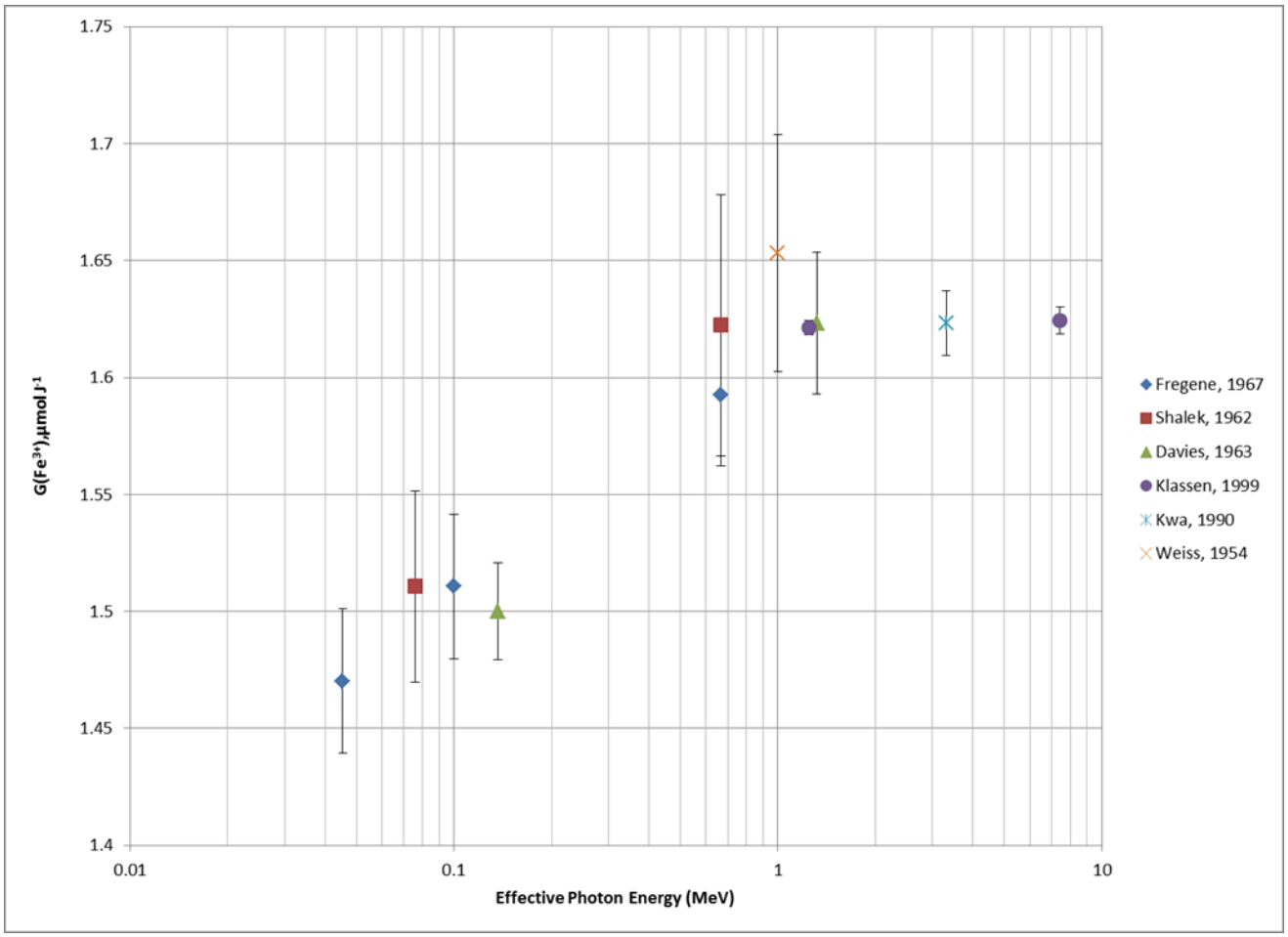

Figure 7 G-value and effective photon energy relationship historical results collected by Klassen (1999)

deals with photons in the range of 0.124 – 1.25 MeV the LET specifier is sufficient over this energy range as demonstrated by figure 7.

Given the dependence of the G-value on the radiolysis products of water and LET of the ionizing radiation, high dose rates would be expected to decrease the G-value by the same mechanisms as high LET radiation. Investigations into the effects of the dose rates of photons showed that the G-value was constant at instantaneous dose rates below 10^7 Gy min^{-1} (ICRU 34, 1982).

2.6 Dose to water determination

The quantity of interest for a dosimeter is the dose to water at a given position. For a Fricke dosimeter an expression for the dose to water may be expressed using the following equations depending on whether the Fricke dosimeter is considered to be a large volume or small volume detector:

$$D_w = D_f \left(\frac{\mu_{en}}{\rho}\right)^{water}_{Fricke} \qquad (2.12)$$

$$D_w = D_f \left(\frac{\bar{L}}{\rho}\right)^{wall}_{Fricke} \left(\frac{\mu_{en}}{\rho}\right)^{water}_{wall} \qquad (2.13)$$

where, $\left(\frac{\mu_{en}}{\rho}\right)^{water}_{Fricke}$ denotes the ratio of mass energy absorption coefficients for water and Fricke solution and $\left(\frac{\bar{L}}{\rho}\right)^{wall}_{Fricke}$ is the restricted stopping power ratio of the wall material and the Fricke solution.

Equation 2.12 assumes a large volume detector where all the dose contributing electrons originate within the Fricke dosimeter whilst equation 2.13 assumes a small volume detector and employs Bragg-Gray cavity theory to account for electrons originating in both the detector wall and the surrounding medium (Ma et al, 1993). The dosimeter is in reality more accurately modeled as somewhere in between these two extremes. Conventionally the dose to water is expressed as a function of dose to the Fricke solution as:

$$D_w = D_f \cdot f_{w,f} \cdot P_{wall} \cdot k_{dd} \,, \tag{2.14}$$

$f_{w,f}$ is a correction factor that accounts for the different radiation absorption properties of the Fricke solution and water. It is calculated as either a ratio of mass energy absorption coefficients for photons or an electron stopping power ratio for electrons (Ma et al, 1993). Since this work only deals with photon irradiations the value of $f_{w,f}$ used ranges from 1.003 - 0.979 depending on the beam quality used, which is close to unity as would be expected given that Fricke solution is closely water equivalent.

P_{wall} corrects for the perturbation, scattering and attenuation of the primary beam photons caused by the material used to hold the Fricke during irradiations (Ma,1992). Glass gives a higher correction factor but is often preferred as it is easier to clean, reducing contamination effects on the optical density readings, whilst plastics being more water equivalent, give smaller correction factors but are more difficult to clean resulting in contamination effects on the optical density measurement. Plastics were used throughout this work to hold the Fricke during irradiations after other work demonstrated

that control measurements adequately correct for contamination effects (Cojocaru et al, 2010).

By using plastic holders in phantom, Fricke dosimeters demonstrate smaller perturbation on dose distributions when compared with ion chambers of similar dimensions (Blazy et al, 2006).

The dose non-uniformity correction factor, k_{dd} , corrects for the dose not being constant over the Fricke solution volume. The correction factor may be obtained from measured 3 dimensional depth dose profiles or by modeling the source using a radiation transport code. The dose non-uniformity correction factor is of particular importance in regions of high depth-dose gradients like the vicinity of a brachytherapy source.

2.7 Conclusion

Providing the uncertainties on the correction factors and the G-value are minimized, the Fricke dosimeter has the potential to provide highly reproducible and accurate results in addition to having a linear dose response in the dose region of interest. Comparisons of Fricke dosimetry and calorimetry absorbed dose standards at Cobalt-60 energies have shown agreement to within 0.1% (Chauvenet et al, 1997).

Fricke dosimetry has seen several applications including its use as a mail order dosimeter (Olzanski et al, 2002) and its use by the Swiss national standards laboratory, METAS, as its primary absorbed dose standard for 5.4-22 MeV electron beams.

As per the TG-43 update guidelines the Fricke dosimeter shows a well characterized energy response in the energy range of interest and its use as a primary standard shows it is capable of the desired precision and accuracy. In addition the requirement for a small active volume can be easily satisfied by manufacturing a holder to encapsulate a small volume of Fricke solution.

3 Chapter: G-value determination

3.1 Introduction

In order to determine the absorbed dose to water at the reference position for an Ir-192 brachytherapy source using Fricke dosimetry the Ferric ion G-value must be determined. To determine the G-value at a given photon energy a knowledge of the dose delivered to the Fricke is necessary. Since the absorbed dose to water at Ir-192 energy is the quantity of interest the G-value cannot be directly determined. To overcome the need to use the dose to water at Ir-192 energy the G-value will be interpolated from G-values at two different energies. The average photon energy emitted by an Ir-192 source is 0.38 MeV. Unlike most brachytherapy sources iridium has a relatively complex multiline decay spectrum, figure 2. The average photon energy lies between 0.1 and 1.6 MeV, a region on figure 7 that can be approximated by a straight line.

The G-value could have been interpolated directly using the data from the literature shown in figure 7. However, the graph shows that the literature in the energy range of interest is dated. The older data not only has a larger uncertainty than is achievable today but relies on slightly different recipes for producing the Fricke solution in addition to different final concentrations for some of the results. More importantly the older data originate at a time when the significance of contamination was not fully understood and most irradiations were conducted in glass vials. The lack of water equivalence meant that

the P_{wall} correction factor was significant and had to be determined without the use of beam radiation transport codes. To determine the G-value at Ir-192 the G-values at both Co-60 and 250 kVp x-ray energies will be measured. Since both these energies are still on the linear portion of the graph they can be used to interpolate the G-value at the energy of interest. In doing so the G-value determined will be solely based on measurements conducted at the National Research Council and as such be independent of the relatively large uncertainties on G-values in earlier work, particularly at low X-ray energies, <0.2 MeV.

Primary standards for both Co-60 and 250 kVp X-rays are used to determine the dose to water which is then converted to the dose to Fricke at a given energy. Equation 2.9 shows that if the optical density is measured, the denominator in the equation, $[\varepsilon \cdot G(Fe^{3+}) \cdot \rho \cdot d]$, can be evaluated by rearranging the equation as follows:

$$\frac{D_F}{\Delta OD_{net}} = [\varepsilon \cdot G(Fe^{3+}) \cdot \rho \cdot d] \quad (3.1)$$

It is important to note that since the readout procedure and Fricke solution composition used throughout this work do not change, the evaluation of the product $[\varepsilon \cdot G(Fe^{3+}) \cdot \rho \cdot d]$ is sufficient and makes this work independent of the value of the density of the Fricke solution, the molar linear absorption coefficient and optical path length of the cuvettes used in the calculation. For completeness however the G-value will be evaluated and compared to earlier work.

3.2 X-ray experiment setup

The setup in figures 8 and 9 was used to determine the G-value at 250 kVp X-ray energy. A 2.047 mm copper filter was applied to the X-ray tube providing an effective photon energy of 0.126 MeV. The air-kerma rate was evaluated at the start of each irradiation day using the National Research Council`s free air chamber X-ray primary standard. A polyethylene bag, figure 9, containing 4.23-4.28 g of Fricke was placed in the PMMA holder shown, attached to a PMMA frame for support. The polyethylene bag center was placed at 80.00 cm from the X-ray source to allow for a greater dose rate than the conventional 1 m calibration distance. The beam used was circular with a diameter of 72.4 mm to ensure the Fricke solution was within the beam, avoiding edge effects. Confidence in the ability to accurately model the setup using a beam radiation transport code allowed the irradiations to be conducted in air. The free air chamber, FAC, primary standard signal must be corrected for measurements not conducted at 1 m due to differences in scatter, electron loss in the FAC collecting volume and beam attenuation. The polyethylene bag was not brought any closer than 0.80 m to minimize the correction required to the FAC measurement for conducting the irradiations at a different point of measurement (Mainegra-Hing et al, 2008). An air-kerma to dose conversion factor was derived from the simulation to determine the dose to the Fricke solution.

3.2.1 PE bag preparation

The following procedure is used to prepare the PE bags for irradiation and readout:

- The bags are prepared as seen in figure 9 with a mark added at 3.8 cm relative to the top of the bottom seal
- Prior to each use the bag's external surfaces are rinsed with Millipore water and hung to dry
- When ready the bags are cut, below the seal, using ceramic scissors that have been rinsed in Millipore water and dried using compressed nitrogen gas
- The cut bag is placed in the bag holder and the balance zeroed
- The Fricke solution is deposited in the bag from the funnel and the bag weighed such that the Fricke solution mass is between 4.23 g and 4.28 g
- The 3.8 cm mark is placed on the heat sealer rim and the bag sealed
- The time is then recorded and the bag is irradiated
- When the Fricke solution optical density is ready to be read the Bag is rinsed with Millipore water if irradiated in air and ethanol then Millipore if irradiated in phantom
- The bag is dried using compressed nitrogen before being cut below the seal
- The bag is placed in a cardboard bag holder and the solution drawn out using a pipette

Low dose rates are characteristic of X-ray tubes. To increase the effective photon energy of the beam, greater filtration must be added resulting in a lower dose rate. The beam chosen was thus a compromise between beam energy and dose rate. To determine the G-value the source was used to deliver an air-kerma of 11 Gy to the Fricke solution, an irradiation time of 1.67 hours. The ambient room temperature during the irradiation was measured and used to convert the optical density readings to the reference temperature using equation 2.10. For each irradiation day a control bag was filled with Fricke and

read out without being irradiated at the beginning and end of the day. The average optical density reading for the control bags of each day was subtracted from the irradiated optical density readings conducted on the same day to determine the net change in optical density. The Fricke was kept in the control bag for the same amount of time as the irradiations. The experiment was repeated for the same target dose of 11 Gy for different bags and the resulting optical density readings are shown in figures 10 and 11**.** It should be noted that the graph shows the uncertainty associated with the readout procedure, Fricke manipulation procedure and the reproducibility of the irradiation conditions. The two figures show the same experiment repeated a year apart.

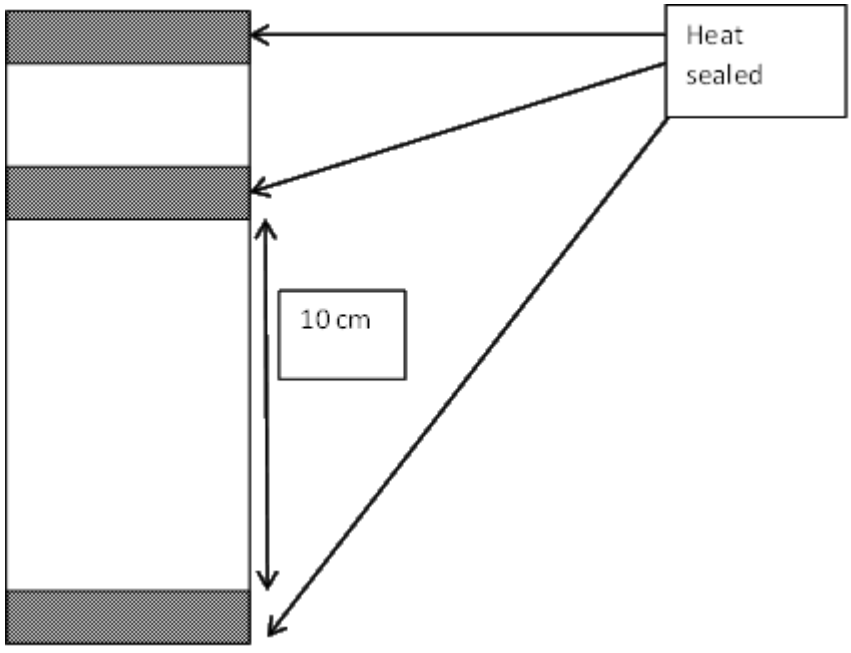

Figure 8 PE bag used to hold Fricke solution

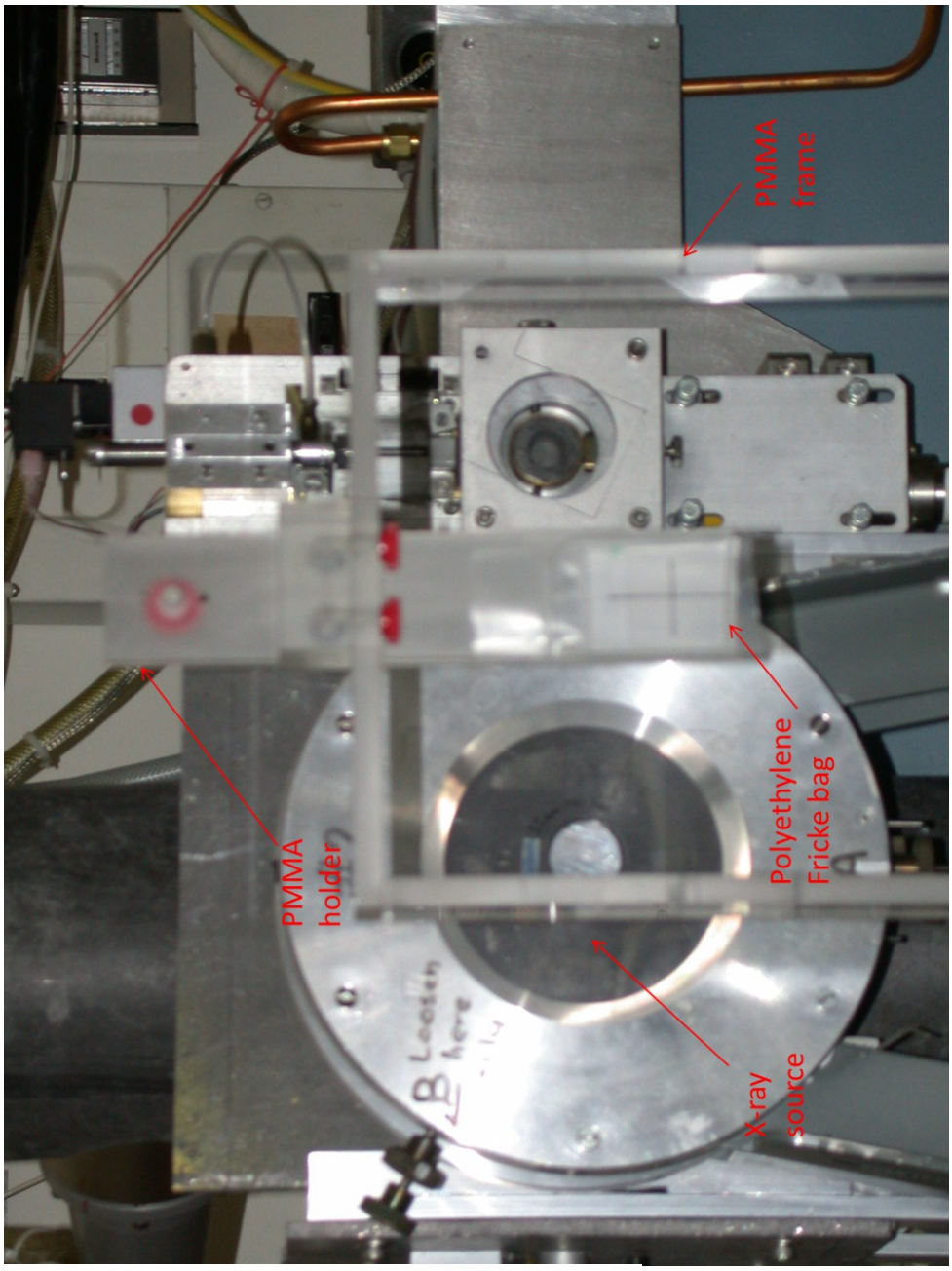

Figure 9 X-ray irradiation setup

The PMMA bag holder has a 0.87 mm thick wall in front of the bag and a 0.93 mm thick wall behind the bag the distance between both walls is 2.97 mm . The side walls are 1.89 mm thick and 43.00 mm apart.

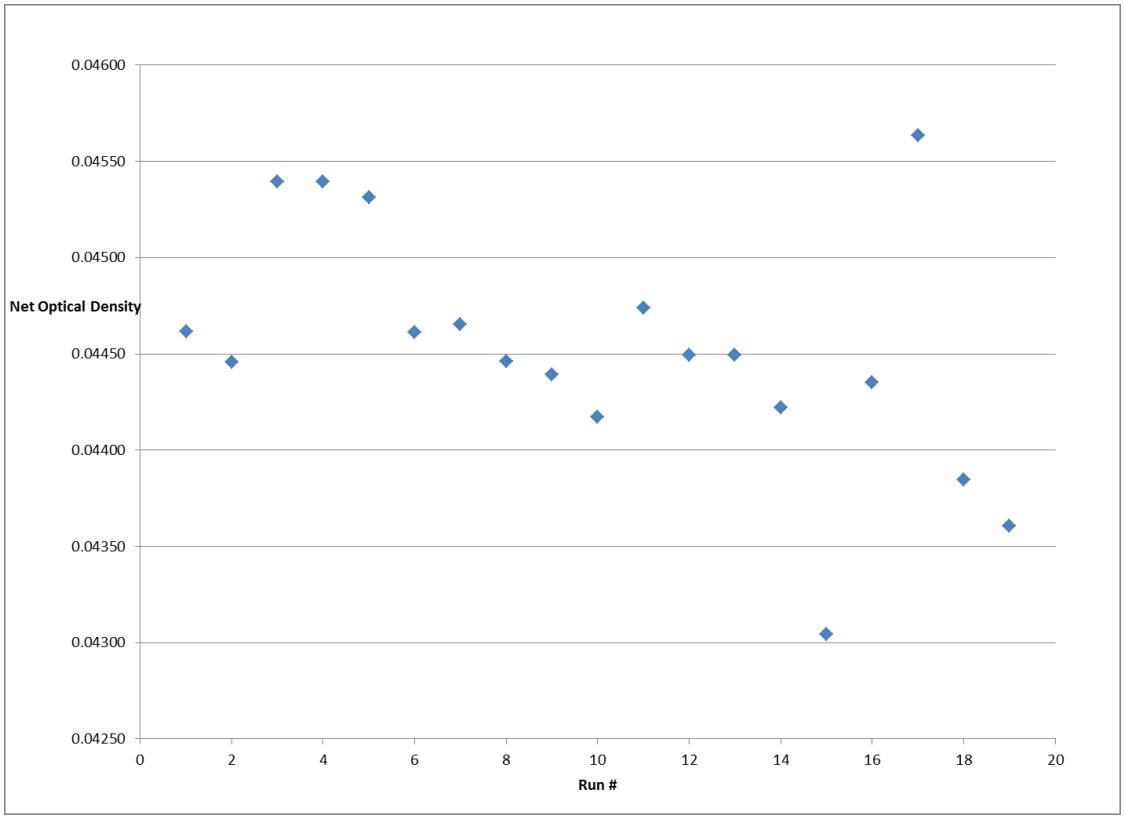

Figure 11 Net optical density results for 2012 250 kVp x-ray irradiations

Similar spread (standard deviation of 0.0006) for both plots

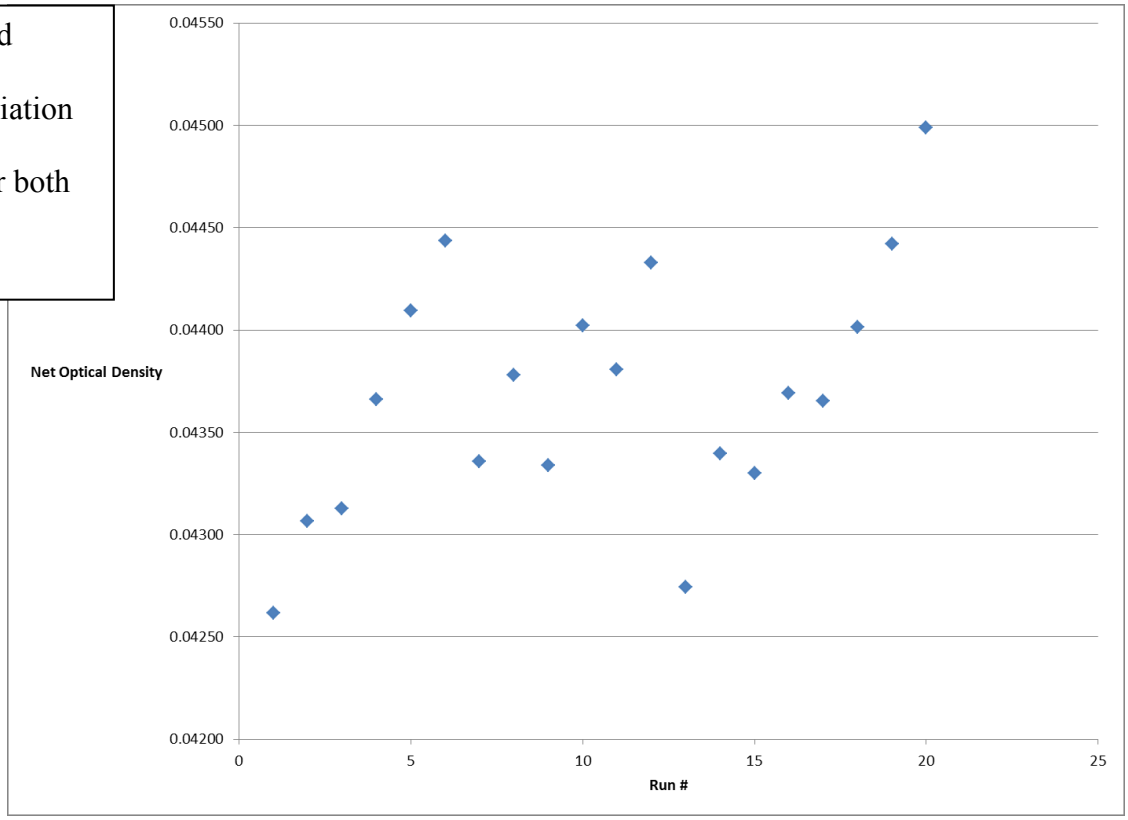

Figure 10 Net optical density results for 2013 250 kVp x-ray irradiations

3.3 X-ray experiment results

To determine the dose to Fricke from the FAC air-kerma measurement a Monte Carlo beam radiation transport simulation was carried out by Dr. Ernesto Mainegra-Hing to account for the scattering effects of both the frame and the holder and the different point of measurement. An air-kerma to Fricke dose conversion factor of 1.154 ± 0.07% (Type A) was obtained. Type A uncertainties are calculated from our measured or simulation data using statistical methods whilst Type B uncertainties include all other uncertainties. The low uncertainty of the correction factor is due in part to an accurate model of the X-ray source used for the irradiations (Mainegra-Hing et al,2008).

The calculated value for $[\varepsilon \cdot G(Fe^{3+}) \cdot \rho \cdot d]$ along with the calculated standard uncertainties (k=1) are shown in the tables below for both series of experiments. The standard uncertainty (k=1) for N measurements is defined as the standard deviation divided by $\sqrt{N}$.

Table 1 250 kVp X-ray G-value experimental uncertainties 2012

	Type A uncertainty	Type B uncertainty	Combined uncertainty	Average Value
$\Delta OD_{25,25}$	0.00021	0.0003	0.0004 (0.8 %)	0.0445
$K_{air\ (Gy)}$	0.005	0.029	0.029 (0.2 %)	11.0
D_F/K_{air}	0.0008		0.0008 (0.1 %)	1.1537
$[\varepsilon \cdot G(Fe^{3+}) \cdot \rho \cdot d]$(Gy^{-1})			3 x 10^{-5} (0.8 %)	0.003508

Table 2 250 kVp X-ray G-value experimental uncertainties 2013

	Type A uncertainty	Type B uncertainty	Combined uncertainty	Average Value
$\Delta OD_{25,25}$	0.00019	0.0003	0.0004 (0.9 %)	0.0437
K_{air} (Gy)	0.005	0.029	0.029 (0.2 %)	10.9
D_F/K_{air}	0.0008		0.0008 (0.1 %)	1.1537
$[\varepsilon \cdot G(Fe^{3+}) \cdot \rho \cdot d]$(Gy^{-1})			3 x 10^{-5} (0.9 %)	0.003475

The results above agree at the 0.9 % level and give an uncertainty on $[\varepsilon \cdot G(Fe^{3+}) \cdot \rho \cdot d]$ of 0.8 %. For completeness the mean G-value is calculated below from the combined experiments.

Table 3 Explicit 250 kVp X-ray G-value uncertainty

	Type A uncertainty	Type B uncertainty	Combined	Average Value
$[\varepsilon \cdot G(Fe^{3+}) \cdot \rho \cdot d]$ (Gy^{-1})			2.1 x 10^{-5} (0.6 %)	0.003492
ρ ($kgcm^{-3}$)		1 x 10^{-7}	1 x 10^{-7} (0.01 %)	1.0227 x 10^{-3}
d (cm)		0.0002	0.0002 (0.02 %)	1
ε (cm^2mol^{-1})		100	100 (0.01 %)	2174000
$G(Fe^{3+})$ (μmol J^{-1})			0.009 (0.6 %)	1.602

An uncertainty of 0.6 % on the G-value at 250 kVp X-ray was obtained. The G-value plotted in figure 14 seems to be much higher than earlier measurements in the literature but with a significantly lower uncertainty.

3.4 Cobalt-60 experiment setup

The cobalt 60 experiment was carried out using the same PMMA holder used for the X-ray experiments. The readout procedure including the cuvettes used was identical. A 30 x 30 x 30 cm water phantom was used for irradiations with the PMMA holder being mounted, figure 12, using the same setup used to calibrate clinical ion chambers at the National Research Council. A source to bag center distance of 1.05 m and a field size of 10 x 10 cm^2 was used, making the field identical to that used to calibrate the cobalt 60 source. The cobalt-60 primary standard was used, with the dose to water being based on the sealed water calorimeter calibration of the source (Shortt et al, 2000). The irradiation time was chosen such that the bags received a dose on the order of 13 Gy to be consistent with the X-ray experiments. The source had a dose rate to water of 714.0 mGy/min for the 2012 experiments allowing the desired dose to be delivered in 20 minutes. To determine the net radiation induced change in optical density of the Fricke solution controls, with the Fricke solution remaining in the bag for the same time as irradiations, were conducted at the beginning of each day and the measured average optical density control value subtracted from all the optical density measurements of the irradiated bags on that day.

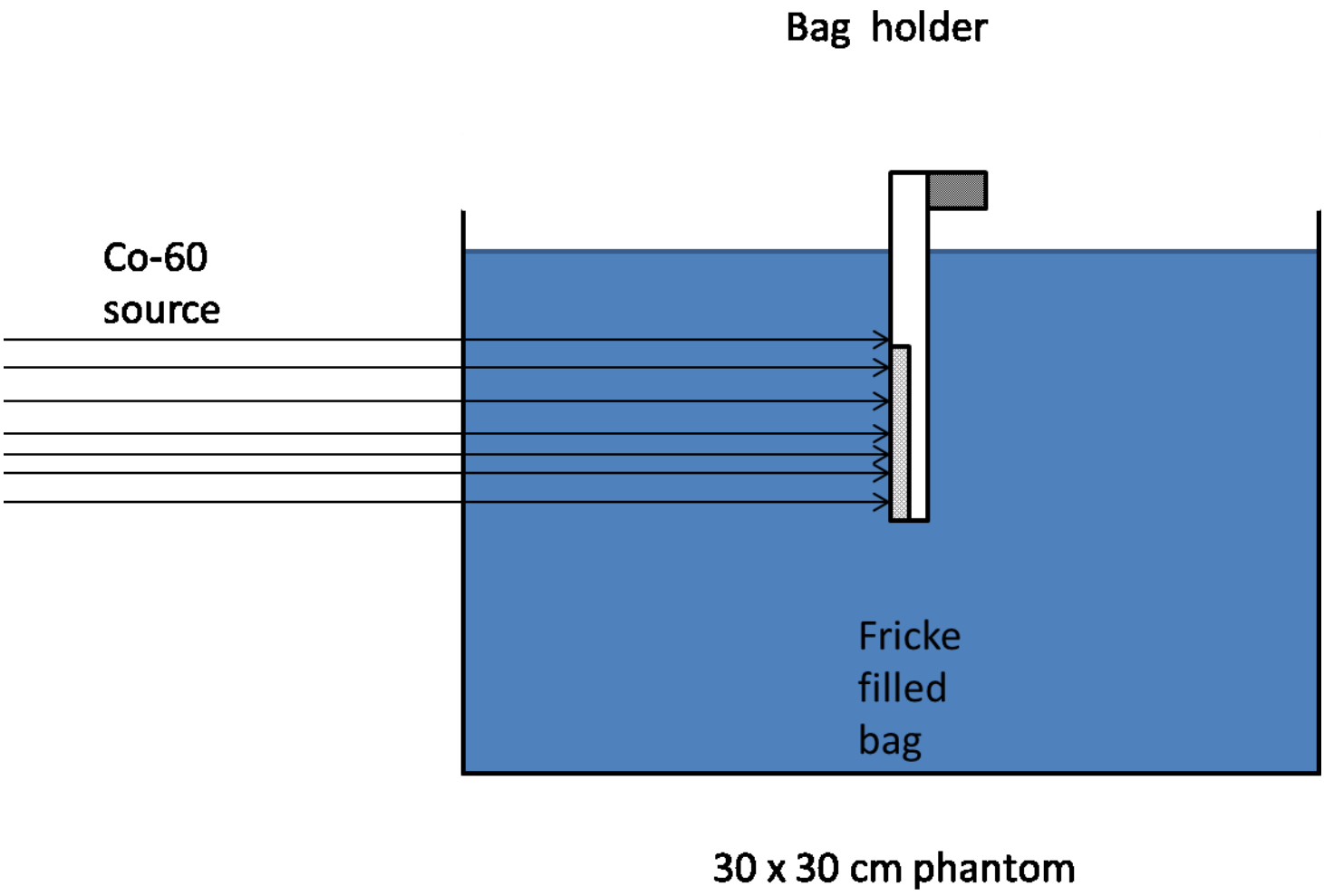

Figure 12 Cobalt-60 G-value experiment setup
The bag center is 15 cm below the phantom water level.

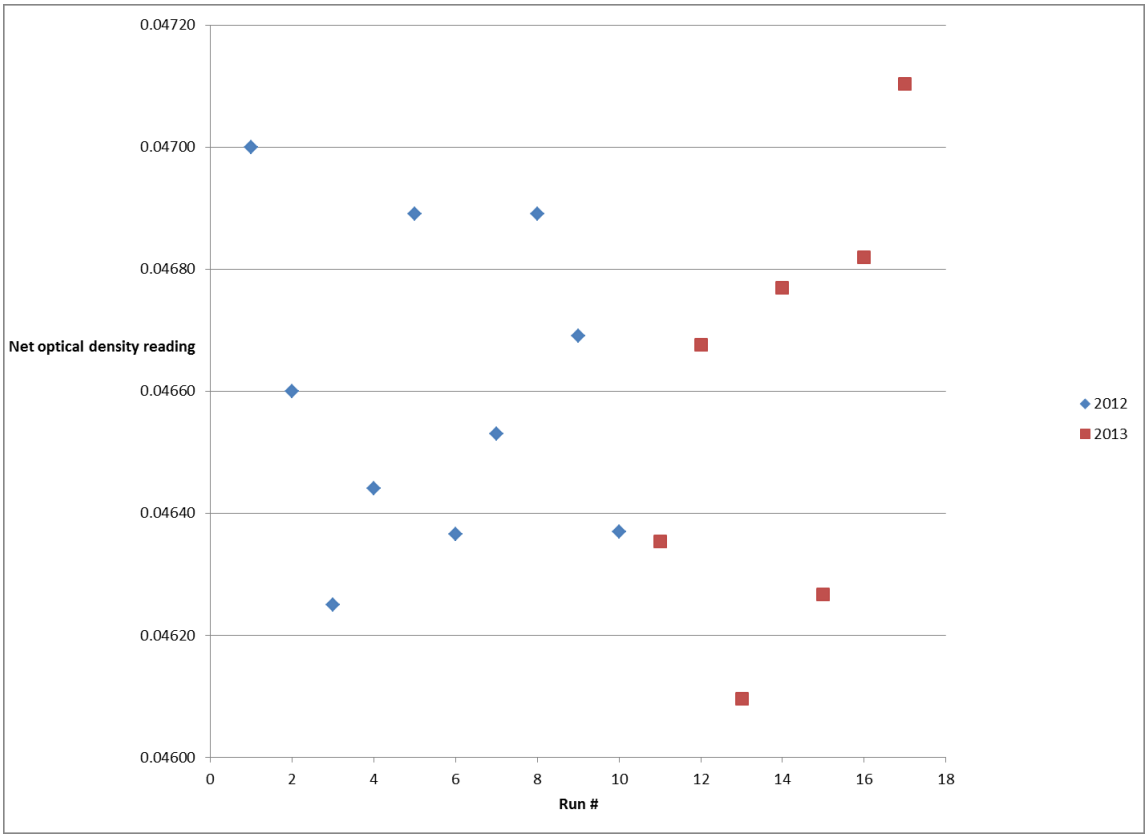

Figure 13 Net optical density readings for Cobalt-60 G-value experiments irradiated for a target dose of 11 Gy

Two experiments were conducted almost a year apart, the resulting net optical density readings for each irradiation day are shown in figure 13.

3.5 Cobalt 60 experiment results

By rearranging equations 2.9 and 2.14 to arrive at the desired quantity,$[\varepsilon \cdot G(Fe^{3+}) \cdot \rho \cdot d]$, the following expression is derived:

$$[\varepsilon \cdot G(Fe^{3+}) \cdot \rho \cdot d] = \frac{\Delta OD_{net} \cdot P_{wall} \cdot k_{dd} \cdot f_{w,f}}{D_w} \quad (3.2)$$

Expression 3.2 is used to derive the uncertainty on the desired quantity. Unlike the X-ray experiment, where a single air-kerma to dose conversion factor was used accounting for all the above correction factors, here they are calculated explicitly, based on a radiation transport code simulation. The results for both cobalt 60 experiments and the associated uncertainties are shown in the tables below, showing agreement at the 0.2 % level.

Table 4 Cobalt-60 2012 experiment results

	Type A uncertainty	Type B uncertainty	Combined uncertainty	Average
ΔOD	0.000087	0.0003	0.0003 (0.6 %)	0.046603
P_{wall}		0.0005	0.0005 (0.05 %)	1.001
k_{dd}		0.001	0.001 (0.1 %)	0.9955
$f_{w,f}$		0.0005	0.0005 (0.05 %)	1.003
D_w (Gy)	0.01	0.01	0.014 (0.1 %)	13.04
$[\varepsilon \cdot G(Fe^{3+}) \cdot \rho \cdot d]$($Gy^{-1}$)			2.3 x 10^{-5} (0.6 %)	0.003572

Table 5 Cobalt-60 2013 experiment results

	Type A uncertainty	Type B uncertainty	Combined uncertainty	Average
ΔOD	0.00018	0.0003	0.0003 (0.6 %)	0.04706
P_{wall}		0.0005	0.0005 (0.05 %)	1.001
k_{dd}		0.001	0.001 (0.1 %)	0.9955
$f_{w,f}$		0.0005	0.0005 (0.05 %)	1.003
D_w (Gy)	0.004	0.01	0.011 (0.1 %)	13.14
$[\varepsilon \cdot G(Fe^{3+}) \cdot \rho \cdot d]$(Gy^{-1})			2.3 x 10^{-5} (0.6 %)	0.003580

Table 6 Cobalt-60 2012 G-value determination

	Type A uncertainty	Type B uncertainty	Combined	Average
$[\varepsilon \cdot G(Fe^{3+}) \cdot \rho \cdot d]$ (Gy^{-1})			2.3 x 10^{-5} (0.6 %)	0.003572
ρ (kgcm^{-3})		1 x 10^{-7}	1 x 10^{-7} (0.01 %)	1.0227 x 10^{-3}
d (cm)		0.0002	0.0002 (0.02 %)	1
ε (cm^{2}mol^{-1})		100	100 (0.01 %)	2174000
G(Fe^{3+}) (μmol J^{-1})			0.010 (0.6 %)	1.610

The G-value for the 2012 readings has been calculated explicitly in table 6 in order to compare the result with previous measurements in the literature. The result agrees with the G-value determined by Klassen et al (1999), of 1.610 ± 0.01 μmol J^{-1}, and lends confidence to the remaining results in this work. The experiment yields a comparable

uncertainty despite being conducted at a significantly lower dose. It should be noted that experiments are typically designed to give optical density readings between 0.2 - 0.5 whilst due to the limitations of the dose rate at 250 kVp X-ray and the short half-life of Ir-192 has meant that all of the optical density readings in this work are within 0.08 - 0.3 . The requirement to achieve results with relatively low optical density readings demonstrates the need to adhere to the strict cleaning protocols developed in this work.

3.6 Ir-192 G-value interpolation

Based on the results of our experiments at cobalt-60, 250 kVp X-ray and the assumption based on historical data that the G-value and effective photon energy have a log-linear relationship in the region of interest a G-value at Ir-192 was obtained. The linear interpolation based on our two standard beams resulted in 1.605 ± 0.005 μmol J^{-1}, figure 14.

Alternatively the quantity $[\varepsilon \cdot G(Fe^{3+}) \cdot \rho \cdot d]$ has a value of 0.00353 ± 2.2 x 10^{-5} Gy^{-1}. An interpolation based solely on the historical data in figure 14 yielded a G-value at Ir-192 of 1.571 ± 0.013 μmol J^{-1}.

The higher G-value at Ir-192 compared to the literature warrants further explanation. Most of the data at low energy, < 1 MeV, were measured before 1970 and it is not clear how the air-kerma to dose conversion factor was calculated, an almost 15 % conversion in our setup. Furthermore different investigators used

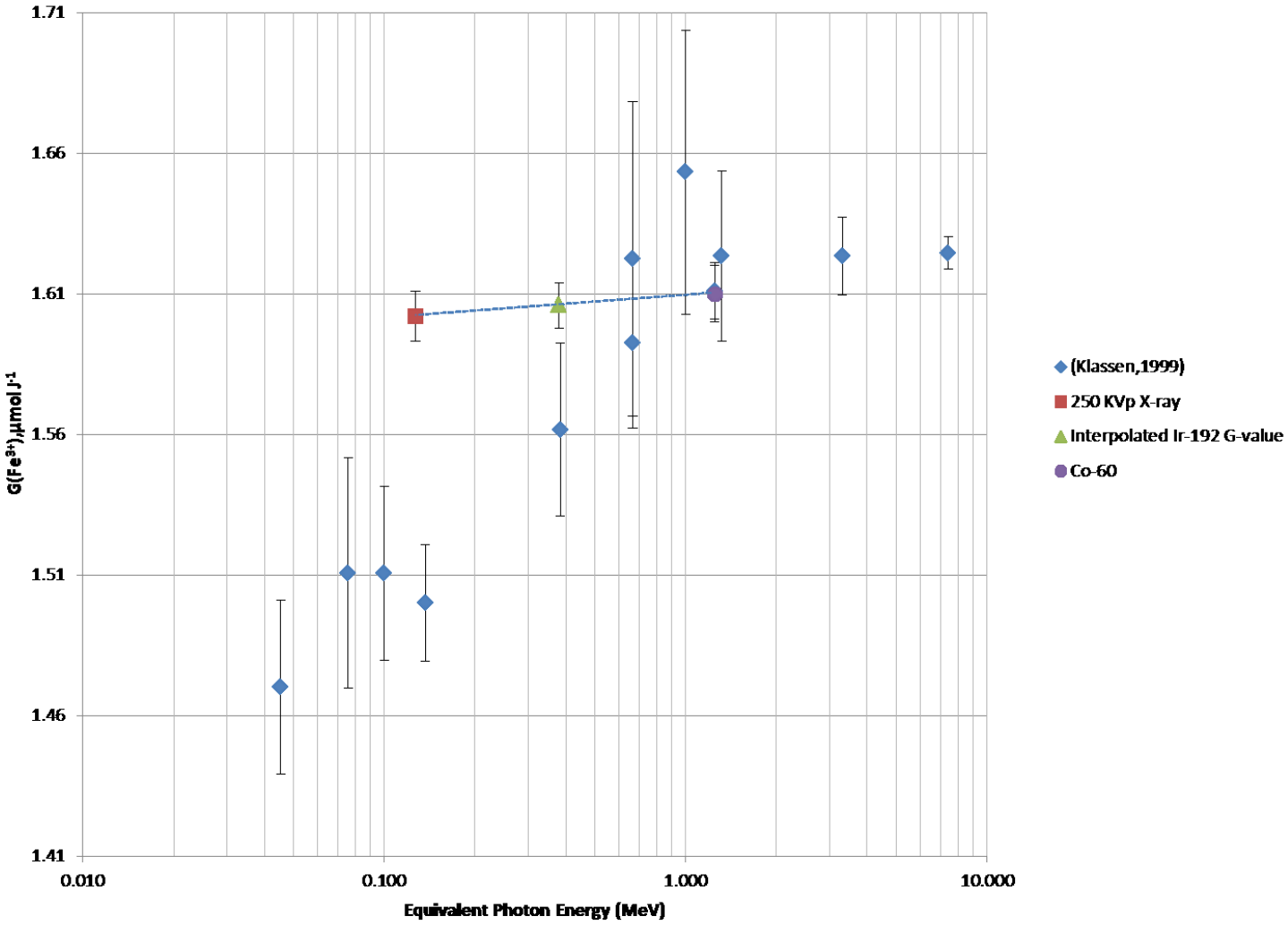

Figure 14 G-value experiment results compared to historical data collected by (Klassen et al , 1999)

different concentrations of Fricke and to account for this some of the data were corrected by 2 % (ICRU 14, 1969), without clear justification. Also, the sensitivity of the Fricke solution optical density readings to contamination was not fully understood at the time. The inability to handle the effects of contamination meant that almost all irradiations were conducted in glass vials with significant P_{wall} correction factors that had to be taken into consideration without the use of radiation transport codes. Finally the good agreement of our Co-60 results with more recent work at NRC (Klassen et al, 1999) lends confidence to the result obtained here.

3.7 Conclusion

An independent determination of the G-value at Ir-192 energy was achieved using only NRC primary standards. Using the same readout procedure throughout this work has meant that the quantity $[\varepsilon \cdot G(Fe^{3+}) \cdot \rho \cdot d]$, 0.00353 ± 2.2 x 10^{-5} Gy^{-1}, can be used to determine the dose to water at Ir-192 making it independent of the uncertainties on the optical path length of the cuvettes, the molar linear absorption coefficient and the Fricke density.

4 Chapter: Ir-192 dosimetry: development of experimental setup

4.1 Introduction

To irradiate Fricke solution in the quantity of interest, water, using an Ir-192 brachytherapy source, a holder to contain the Fricke and a method of aligning the source with the holder needs to be developed. For the irradiations to be successful the holder must isolate the Fricke from the surrounding water in the phantom, have the capacity to hold enough Fricke for a successful readout and not chemically contaminate the Fricke affecting the optical density readings.

4.2 Holder development

PE bags used for Co-60 and X-ray irradiations were not used due to the large dose non-uniformity correction factor involved. To minimize this large correction the source to bag distance would have to be increased resulting in a lower dose rate and hence a smaller change in the optical density readings resulting in greater sensitivity to contamination.

In the initial development phase we therefore attempted to use a ring shaped holder design used by Austerlitz et al (2008). The ring shaped Poly(methyl methacrylate), PMMA, holder shown in figure 15 was covered with Parafilm M™ (Brand, Wertheim), a sealing film made up of polyolefins and paraffin waxes, to separate the Fricke solution from the phantom.

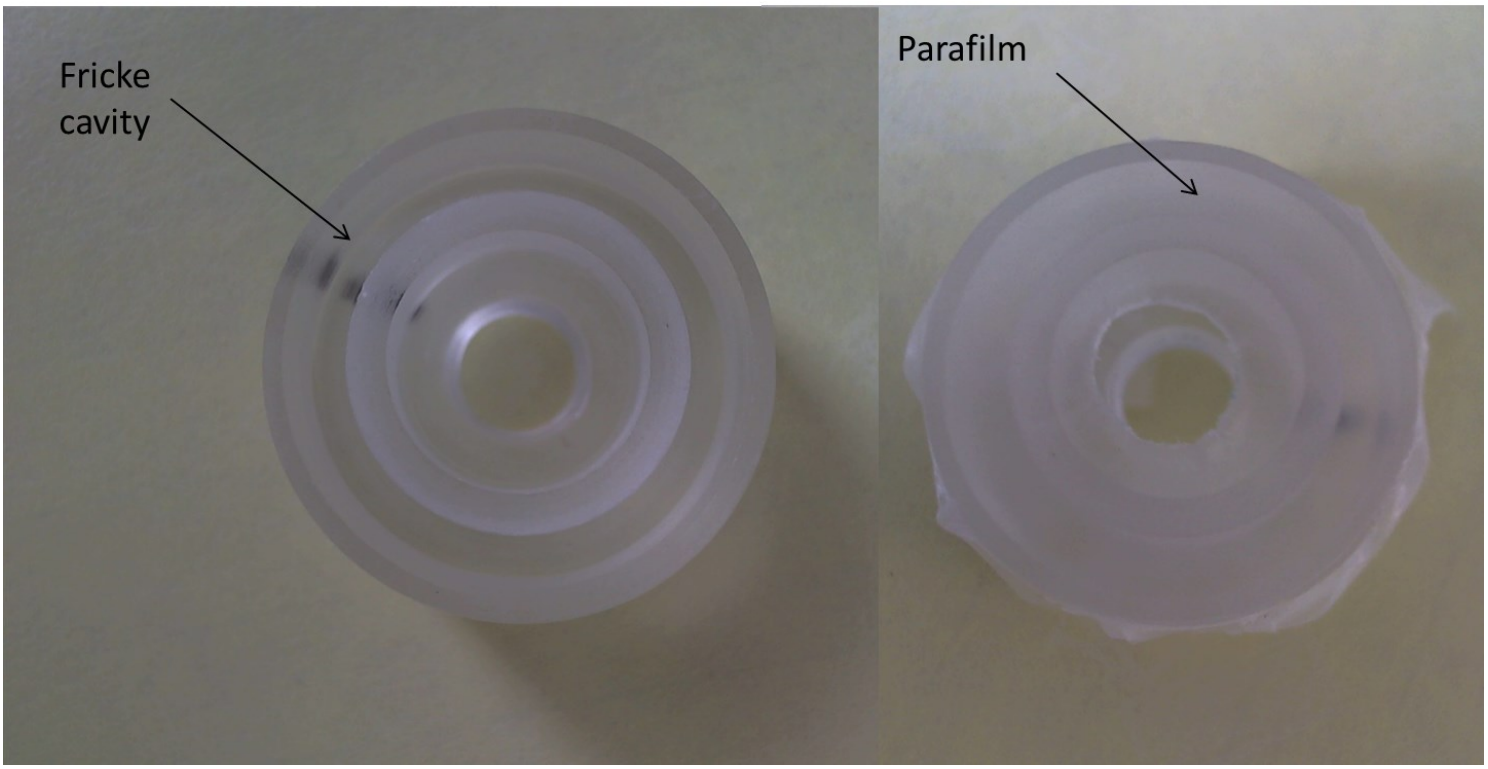

Figure 15 Fricke holder prototype attempt at using Austerlitz parafilm sealing method

A ring shape was chosen by Austerlitz et al to maximize the volume of Fricke around the source whilst minimizing the dose-drop off over the solution volume with transverse distance from the source. PMMA was used primarily for its ease of machining and close water equivalence compared to glass vials conventionally used for Fricke irradiations. Initial experiments showed that using the Austerlitz holder significantly contaminated the Fricke solution producing optical density readings that were not reproducible.

To determine the cause of the contamination, irradiations were conducted in air using the same holder without the Parafilm M™ sealing film. This resulted in a standard uncertainty on our average optical density readings, for irradiations conducted for 10 minutes and corrected for source decay, of 0.24 % for 14 readings (a standard deviation of 0.8 %). The increased reproducibility of the measurements showed that the Parafilm M™ sealing film was significantly contaminating the Fricke solution. To overcome this a Teflon ring, cut from a 0.08 mm Teflon sheet, was placed between the film and the Fricke with a PMMA cap being used to ensure a water tight seal, figure 16**.**

4.3 Irradiation setup

The setup in figures 17 and 18 was developed for irradiations. A Nucletron microSelectron ™ (Elekta, Stockholm) unit was used to deliver a microselectron V2 Ir-192 seed through a Proguide sharp catheter™ (Elekta, Stockholm). The catheter is placed within a PMMA guide tube which the Fricke holder can be fixed to using a delrin stopper, figure 19.

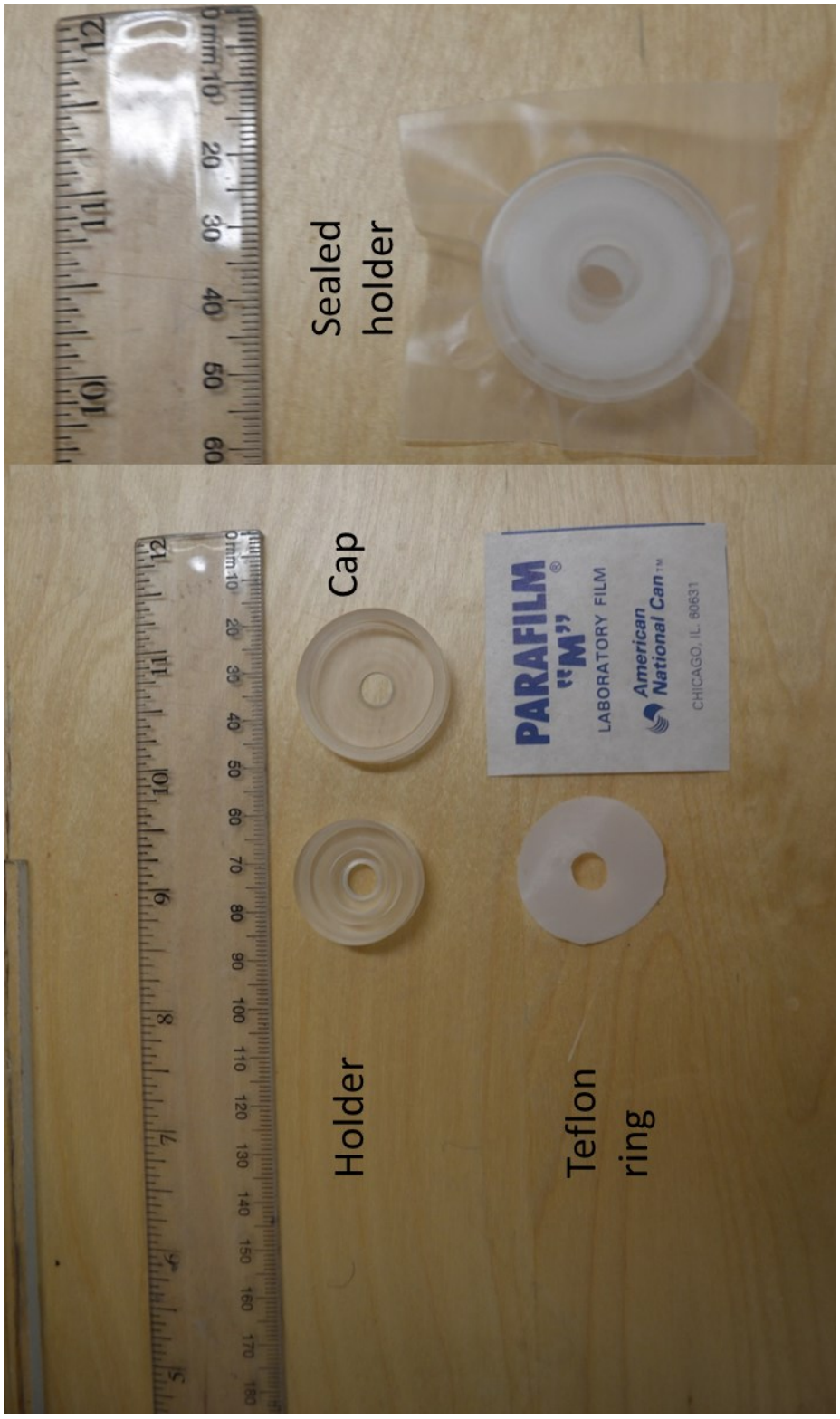

Figure 16 Final holder design showing the sealing apparatus used

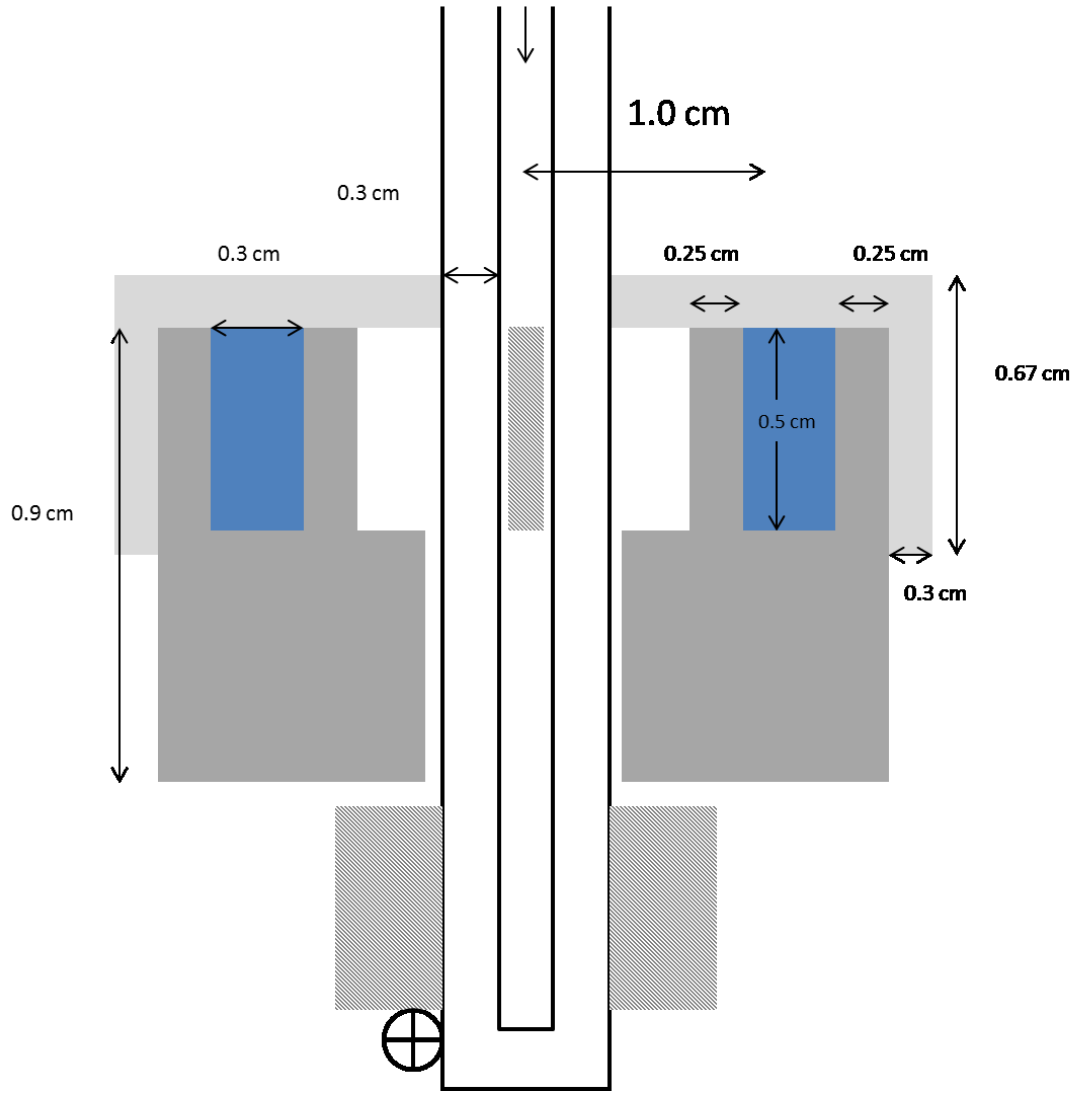

Figure 17 Holder dimensions

For clarity the Parafilm M ™ and Teflon seals are omitted from the diagram in addition to the catheter. All unshaded components maybe modeled as water.

A 15 cm diameter and 15 cm deep circular water phantom was used for irradiations and can be raised to adjust the holder depth within the phantom.

A radiation transport simulation conducted by Ernesto Mainegra-Hing justified the use of such a small phantom by showing corrections of less than 0.1 % when increasing both the phantom radius and depth by 15 cm and 10 cm respectively. The largest correction the simulation yielded was for the holder depth showing a 0.22 % correction for the holder being placed off center, along the vertical or Z axis, by 5 cm in either direction. The energy of the Ir-192 photons explains the simulation results as photons that backscatter back into the phantom at the edge or scatter into the surrounding environment will not reach the holder.

4.4 Source positioning

For this setup to yield reproducible results the position of the source center needs to be determined. Several approaches were investigated. Preliminary experiments using XR/QA Gafchromic (Ashland, Covington) film, where the catheter was taped to the film before irradiating, provided insufficient resolution, figure 20, to accurately determine the position of the seed center.

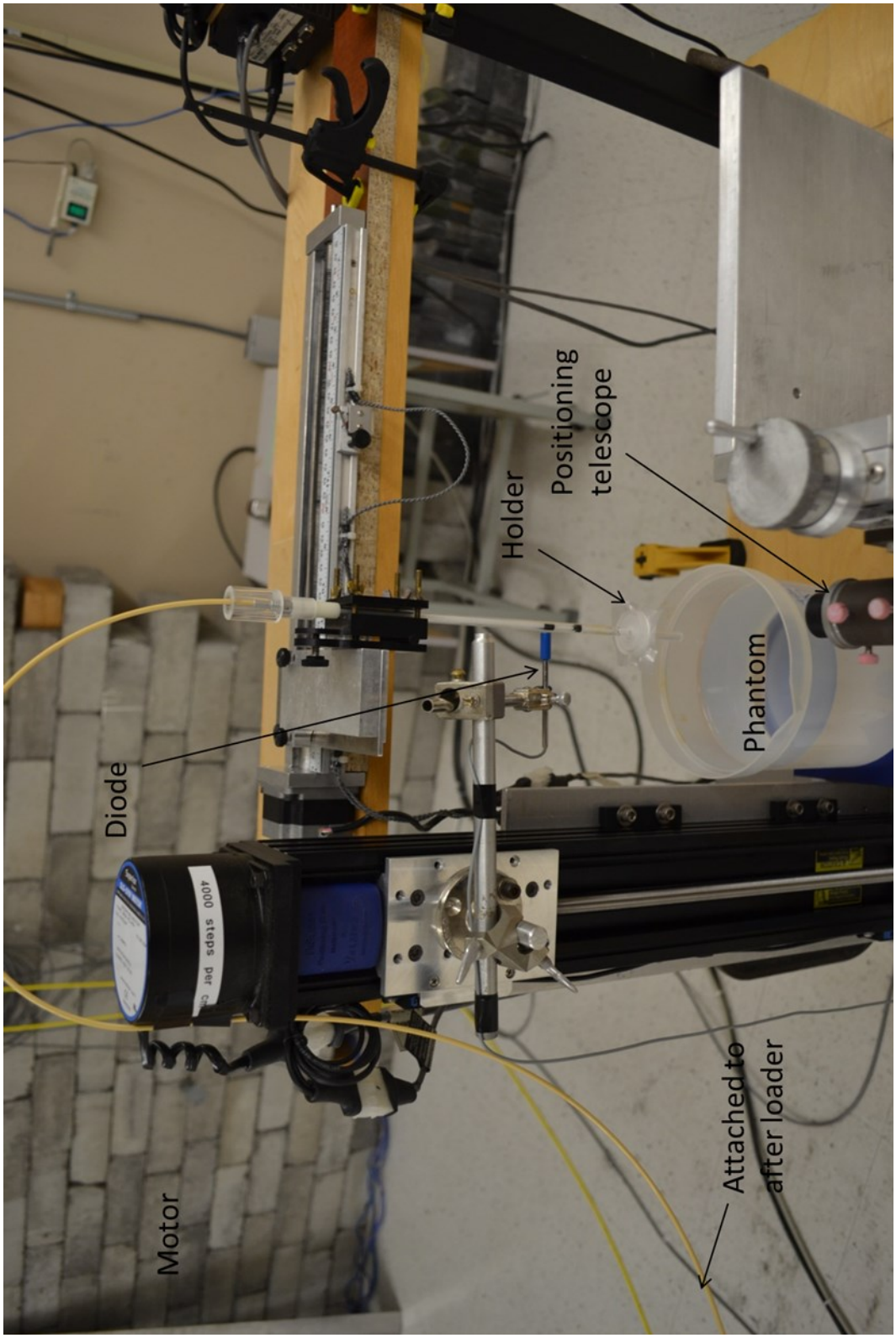

Figure 18 Ir-192 irradiation setup

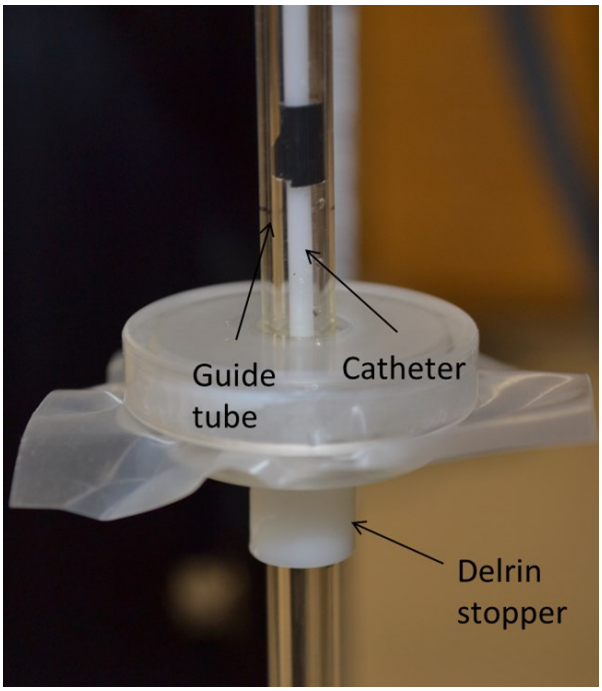

Figure 19 Mounted Fricke holder

Another approach was to use a remotely operated camera to take a picture of the seed once it had reached its final dwell position. By using marked graph paper as a point of reference the position could be determined. Unfortunately as figure 21 demonstrates, due to the translucent nature of the catheter and the need to take apart the irradiation setup prior to each reading this method was abandoned.

Further attempts were made to determine the seed position using ion chambers and diodes. To achieve this a detector was mounted on a motor that allowed the operator to scan the length of the guide tube, figure 18. The table below shows a list of the detectors investigated.

Table 7 Ion chambers and diode detectors investigated to determine seed centre positioning

Detector + Serial number	**Type**	**Sensitive volume**
PTW-60012-0161	Diode	0.0025 mm^3
A16-43375	Ion chamber	0.07 mm^3
IBA-SFD-1506	Diode	0.11 mm^3
IBA-EFD-2753	Diode	0.38 mm^3

The IBA-EFD-2753 diode was eventually chosen over the remaining detectors. Although the diode had the largest sensitive volume it subtends a small solid angle, compared to its sensitive volume size, relative to the seed. Experiments showed that the diode was able to determine the position of the seed with a resolution of ± 0.1 mm, figure 22.

For convenience the diode measurements were conducted in air, with the phantom lowered. By assuming the position of maximum diode signal occurred when the center of the diode was aligned with the center of the seed a telescope can be used to determine the position of the seed center, figure 18. The telescope can then be used to position the holder such that the seed center is aligned with the center of the Fricke cavity. The determination of the seed position was done once at the beginning of each irradiation day even if the source position was not changed from the previous day. Throughout this work the seed position was observed to vary by less than 0.5 mm. Larger changes in seed position between 0.5 – 0.7 mm were only observed when the after-loader treatment plan was changed while the dwell position was kept the same.

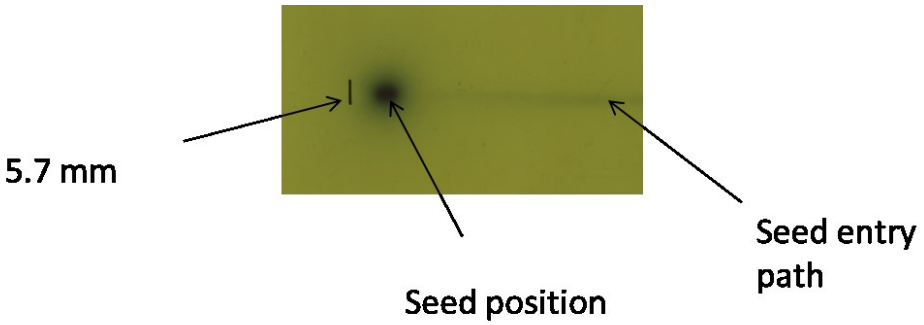

Figure 20 Attempt to determine seed position along the catheter using Gafchromic film

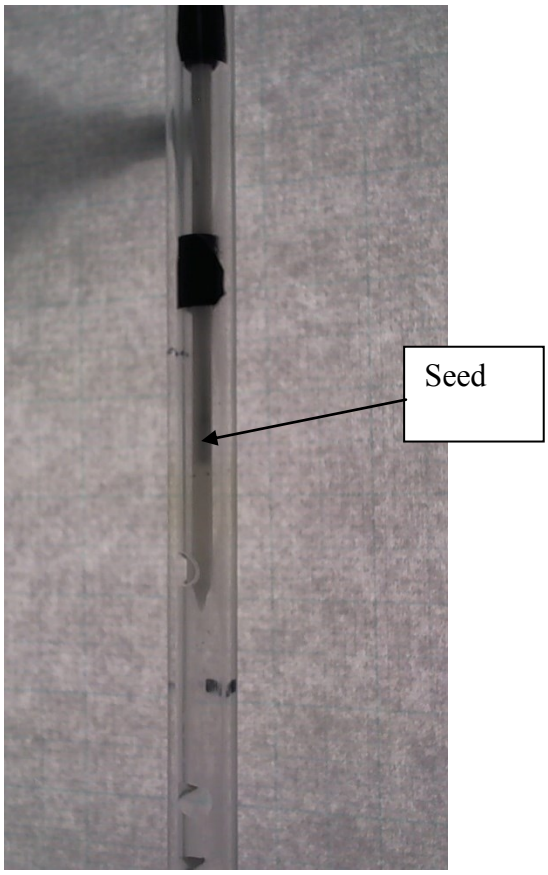

Figure 21 Attempt to use a camera to determine seed position along the catheter

4.4.1 Holder cleaning procedure

- A Teflon ring is cut by making a hole using a stamp and then tracing the outline of the cap using a blade
- The Teflon ring is stored in a beaker filled with 95.5 % sulfuric acid
- The holder is rinsed and dried using Millipore water and the aspirator 5 times
- The cap is rinsed and dried 5 times using Millipore water and the aspirator
- The holder is rinsed and dried 3 times using Fricke solution from the funnel
- The holder is filled with Fricke solution
- The Teflon ring is rinsed 15 times using Millipore water and dried using compressed nitrogen gas
- The Teflon ring is used to cover the Fricke holder
- A stamp is used to cut a hole in the middle of a square of Parafilm M™
- The Parafilm M™ is placed on top of the Teflon ring, to make taking the holder apart easier, and the entire holder is covered using the cap
- Once the device is irradiated the solution is transferred using a pipette for the readout procedure which is identical to that used throughout this work

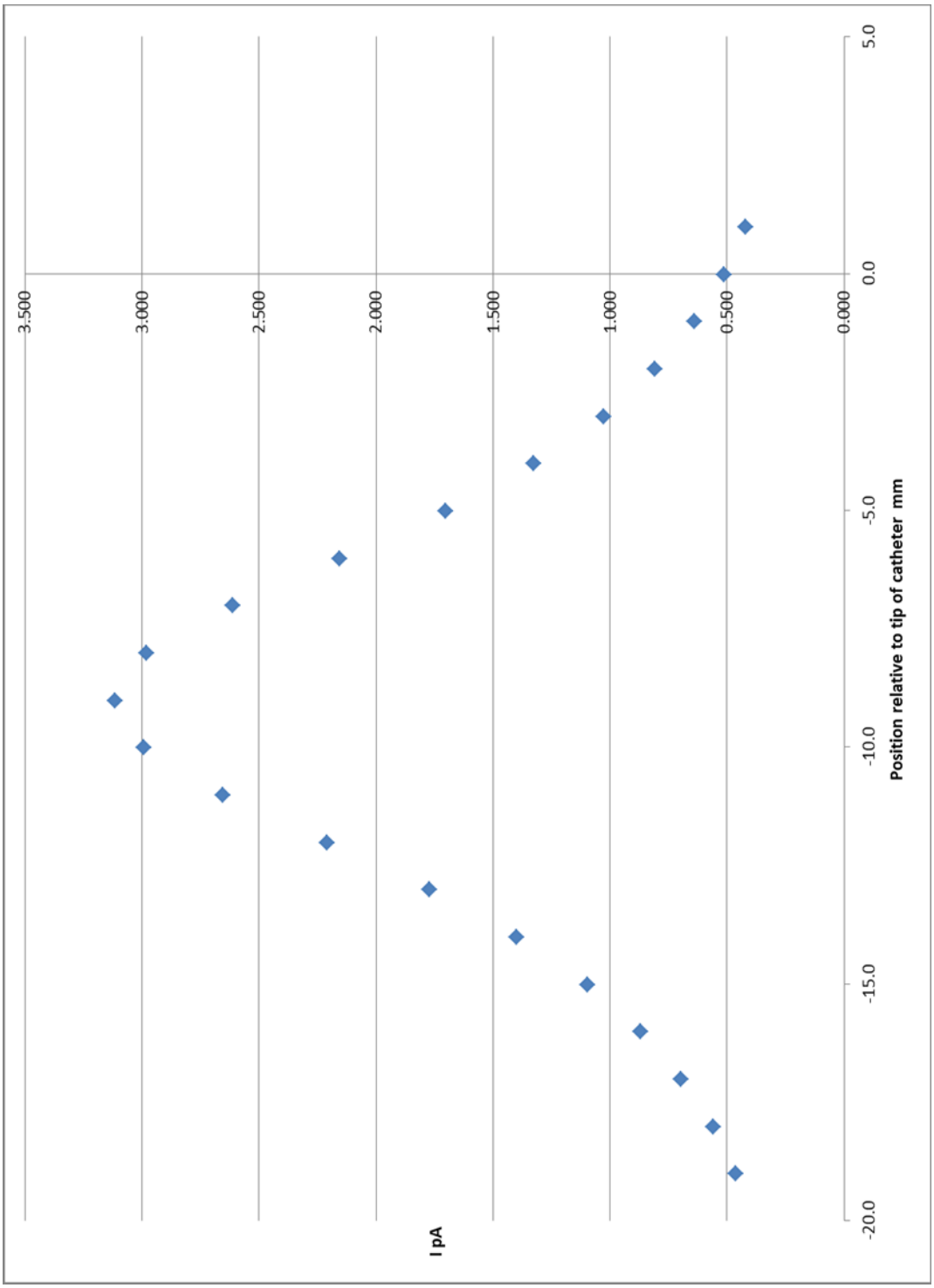

Figure 22 Sample diode scan to find Ir-192 seed center

Irradiations were conducted for a fixed amount of time, 10 minutes typically for a hot source ≈ 360 GBq , and corrected for source decay so that each absorbance measurement reflected the effect of the same dose on the Fricke solution. Control measurements were conducted whereby the entire procedure would be repeated without irradiating and the average control reading subtracted from each irradiated one to account for any holder contamination effects. This resulted in a standard uncertainty of 0.29 % and 0.14 % on the net absorbance and control values respectively for 22 runs. A standard deviation on the net absorbance readings of 1.4 % was achieved.

4.5 Conclusion

This preliminary experiment resulted in several modifications to our procedure:

1. Fricke solution would no longer be kept in the glass funnel on the lab bench for more than a week due to evaporation affecting Fricke solution concentration resulting in an increase in the absorbance of the unirradiated Fricke solution
2. To account for any funnel storage effects, controls would be taken each day
3. The catheter would be replaced after a maximum of 30 irradiations due to observed radiation damage

The high reproducibility of the optical density measurements demonstrates the feasibility of using the procedure to determine the absorbed dose to water at the reference position independently of air-kerma at Ir-192 energy. Based on the modification to the procedure

further irradiations were conducted with the aim of establishing the dose to water at the reference position.

5 Chapter: Dose to water at the reference position

5.1 Introduction

With the G-value at Ir-192 having been determined and the procedure for cleaning and irradiating the Fricke holder developed for brachytherapy irradiations two further experiments were conducted with the aim of evaluating $D_w(r_0,\theta_0)$. The experiments were conducted one month apart using the same setup outlined in chapter 4 with the modifications to the procedure cited in section 4.5. The experiments were conducted using the same source and each run involved irradiating the holder for a fixed time of 10 minutes in both experiments. The results of both experiments are outlined in table 8.

Table 8 Final Iridium irradiation optical density results

Date	December 2012	January 2013
Number of runs	6	6
Net optical density	0.2273	0.1581
Standard deviation	0.6 %	1.1 %
Standard uncertainty	0.3 %	0.5 %

Six runs were conducted based on experience which showed that further runs did not result in an appreciably lower uncertainty. The total time using the modified procedure to conduct one run including the irradiation time, associated cleaning and readout was

approximately 2.5 hours. It should be noted that each result in a given experiment would be corrected for source decay relative to the first reading taken in a data set. The lower net optical density readings for January 2013 are a result of source decay.

5.2 Dose to Fricke evaluation

To evaluate the dose absorbed by the Fricke solution the interpolated quantity $[\varepsilon \cdot G(Fe^{3+}) \cdot \rho \cdot d]$ value at Ir-192 energy will be used. Dividing the optical density readings by $[\varepsilon \cdot G(Fe^{3+}) \cdot \rho \cdot d]$, 0.00353 ± 0.00002 Gy^{-1}, will yield the absorbed dose. The dose rate measured by the Fricke solution in the holder for both experiments is shown in table 9. The standard uncertainties (k=1) are quoted in the table.

Table 9 Iridium dose to Fricke measurements

Date	14th December 2012	21st January 2013
D_F (Gy)	64.39 ± 0.44	44.79 ± 0.36

5.3 Experiment setup dose contribution

Before the dose to water was evaluated a radiation transport simulation conducted by Dr. Ernesto Mainegra-Hing to investigate the effects of the individual parts making up the irradiation setup on the absorbed dose was undertaken. The results are shown in table 10.

Table 10 Summary of irradiation setup effect on absorbed dose

Simulation	Contribution to dose	Type A uncertainty (simulation runs only)
Holder material effect	1.0012	0.002 %
Catheter effect	0.9997	0.002 %
Cable effect	1.0001	0.002 %
Dose non uniformity effect	0.9800	0.009 %

The simulation shows that the effects of the setup (holder, catheter, cable) on the absorbed dose to water is less than 0.1 %. In accordance with equation 2.14 the correction factors necessary for the calculation of the dose to water were calculated using the same transport code by Dr. Ernesto Mainegra-Hing with the results summarized in table 11.

Table 11 Fricke correction factors for Iridium setup

	Value	Uncertainty %
$f_{w,f}$	0.9792	0.003
P_{wall}	0.9991	0.003
k_{dd}	1.0227	0.018
Total	1.0005	0.018

Table 11 shows an unintended but fortuitous cancellation of correction factors resulting in an overall correction from D_F to D_w of close to unity.

5.4 Dose to water determination

Using the correction factors in table 11, $D_w(r_0,\theta_0)$ was evaluated for both the December and January measurements and compared to the TG-43 based determination made at NRC. The results are shown in table 12.

The TG-43 determination at NRC is based on a spherical ion chamber used to measure the air-kerma strength at several distances from the source. The main issue with the air-kerma strength measurement is that scatter has to be accounted for as the measurement is conducted in air and not in vacuum and in a finite room. To do this two approaches are used: one involves the use of a lead wedge to block the primary beam such that only scattered radiation reaches the detector and the second models the entire room using a beam transport code. Once the contribution of scatter is determined it can be subtracted from the initial readings to determine the contribution made solely due to the primary beam.

Table 12 Fricke based dose to water determination at the reference position compared to TG-43

	$D_w(r_0,\theta_0)$	TG-43 based $D_w(r_0,\theta_0)$	D_w(Fricke)/D_w(TG-43)
14th December 2012	64.4 ± 0.4 Gy	66.0 ± 0.8 Gy	0.98
21st January 2013	44.8 ± 0.4 Gy	46.2 ± 0.6 Gy	0.97

The results are consistent with each other and agree within the provided uncertainties with the TG-43 based determination conducted at NRC at the 2σ level.

5.5 Best estimate of standard uncertainty

By correcting the January measurements for source decay back to the start date of the December experiment a single data set of 12 readings can be used to provide the best estimate of the standard uncertainty on the dose to water. Table 13 shows the results with the necessary correction factors used to calculate the final standard uncertainty.

Table 13 Uncertainty budget for Fricke based D_w determination

	Value	Uncertainty
$\Delta OD_{average}$	0.2266	0.0007
$[\varepsilon \cdot G(Fe^{3+}) \cdot \rho \cdot d]$ (Gy^{-1})	0.00353	0.000022
$(f_{w,f} \cdot P_{wall} \cdot k_{dd})$	1.0005	0.00019
D_w (Gy h^{-1})	64.2	0.4

The addition of the January measurements fails to appreciably change either the dose or the uncertainty further justifying the use of six runs per data set.

6 Chapter: Conclusion

The aim of this project was to develop an absorbed dose to water primary standard for Ir-192 brachytherapy based on the Fricke dosimeter. To achieve this within the framework of the existing TG-43 protocol a determination of the absorbed dose to water at the reference position, $D_w(r_0,\theta_0)$, was undertaken. Prior to the measurement of $D_w(r_0,\theta_0)$ the radiation chemical yield of the ferric ions (G-value) at Ir-192 energy was established. This was done by determining the G-value at Co-60 and 250 kVp X-rays with the absorbed dose at each energy being determined using NRC's primary standards. The G-values at Co-60 and 250 kVp X-rays were found to be 1.610 ± 0.010 μmol J^{-1} and 1.602 ± 0.009 μmol J^{-1} respectively. Using the two aforementioned G-values a log-linear interpolation was used to determine a G-value at Ir-192 energy of 1.605 ± 0.005 μmol J^{-1}.

An irradiation geometry was subsequently developed in addition to a holder to contain the Fricke solution and allow irradiations in phantom to be conducted using an Ir-192 brachytherapy source. Once the geometry and holder were optimized two experiments were undertaken to determine $D_w(r_0,\theta_0)$. The $D_w(r_0,\theta_0)$ Fricke based results agreed within uncertainties with the TG-43 air-kerma based values at the 2σ level.

The relative standard uncertainty of the Fricke based $D_w(r_0,\theta_0)$ determination was 0.7 %, due to the ability to control contamination, an irradiation geometry that didn't significantly contribute to the dose and small correction factors compared to TG-43. The

determination of the G-value is the dominant source of uncertainty in this work. A more accurate determination of the G-value at Ir-192 energy would make a Fricke based absorbed dose to water primary standard with a significantly lower uncertainty possible.

The G-value presented in this work for 250 kVp X-rays was significantly larger than earlier, pre-1970, values in the literature although it has a lower uncertainty. The higher G-value at Ir-192 compared to the literature warrants further explanation. Most of the data at low energy, < 1 MeV, were measured before 1970 and it is not clear how the air-kerma to dose conversion factor was calculated, an almost 15 % conversion in our setup. Furthermore different investigators used different concentrations of Fricke solution and to account for this some of the data was corrected by 2 % (ICRU 14, 1969), without clear justification. Also, the sensitivity of the Fricke optical density readings on contamination was not fully understood at the time. Ideally a determination of the G-value at a beam quality between Co-60 and 250 kVp X-ray would reduce the uncertainty on the G-value at Ir-192 and lend further confidence to our results.

Despite the concern regarding G-values at kV X-ray energies, the ability to perform a Fricke based absorbed dose to water determination for brachytherapy serves to verify the accuracy of the TG-43 based standard and has the potential to be further developed to provide an even lower uncertainty on $D_w(r_0,\theta_0)$.

Appendices

Appendix A Cleaning apparatus

A.1 Pipette Cleaning

The 9 inch borosilicate glass pasteur pipettes used throughout this work to transfer the Fricke solution from the irradiation vessels to the cuvettes must be cleaned in accordance with a strict protocol. The following steps are used to prepare a batch of 30 pipettes for use. The apparatus used is shown in figures 23 and 24 :

- A large beaker is rinsed 5 times with Millipore water and placed below cleaning beaker drain
- The pipettes are placed in the cleaning beaker
- 95.5 % sulphuric acid is added to the cleaning beaker up to 1 cm below the pipettes
- The pump is turned on allowing the acid to circulate through the pipettes
- More acid is added until the acid level covers roughly half the length of the pipettes
- The pump is switched off and a valve isolates it from the acid
- A Bernoulli pump is switched on to allow the pipettes to suck up the acid until no air is left inside the pipette
- The Bernoulli pump is switched off and the circulation pump switched back on
- The circulation pump is left to run for 4 hours

- The acid is then drained into the beaker and disposed of
- The procedure is then repeated five times using Millipore water instead of acid for a shorter circulation time of 30 minutes
- Before a pipet is used 1.5 L of Millipore is run through it and the tip is cleaned using a Millipore filled beaker
- The pipette is then dried for approximately 15 minutes using compressed nitrogen gas.

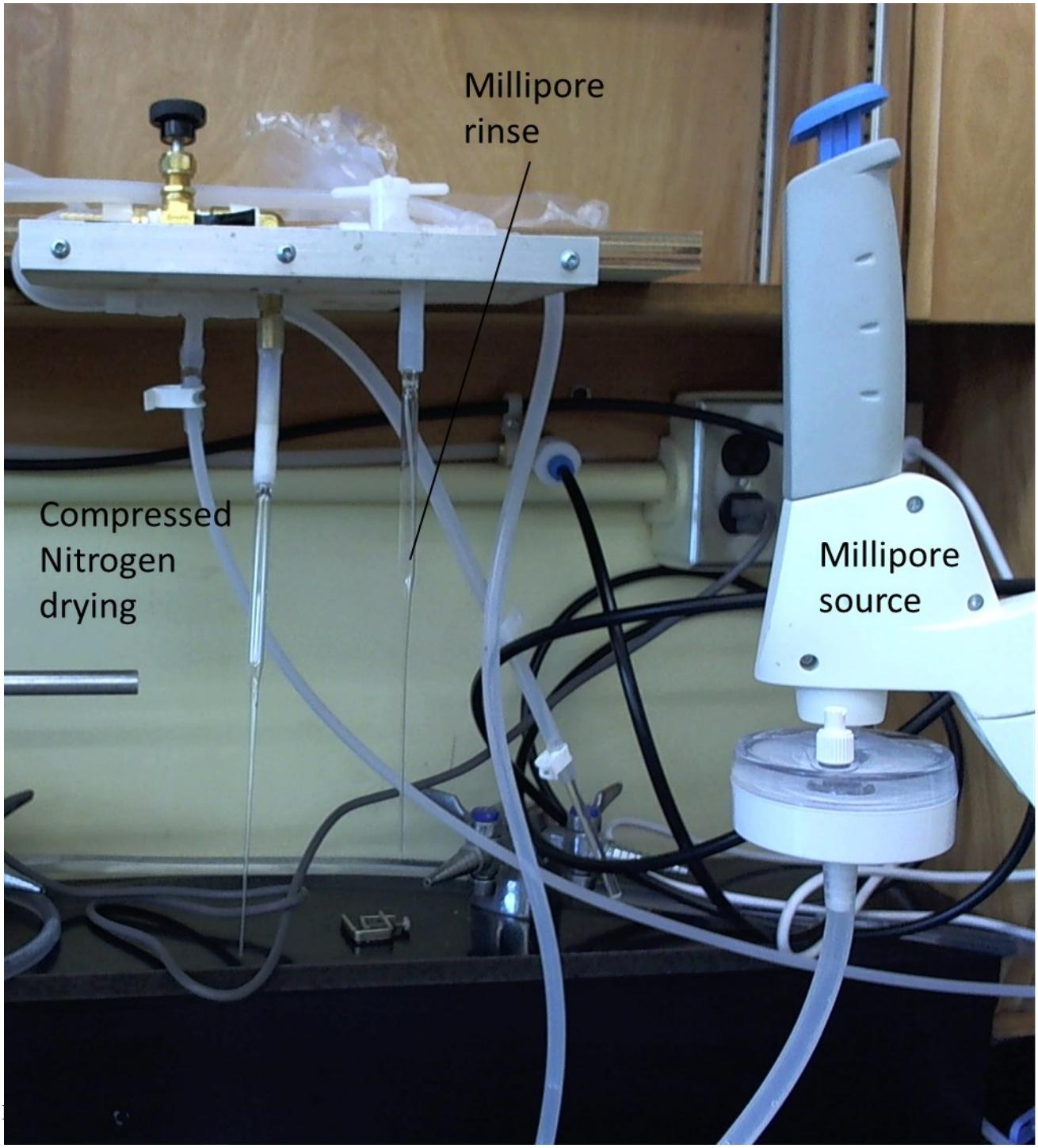
Millipore
rinse
Compressed
Nitrogen
drying
Millipore
source

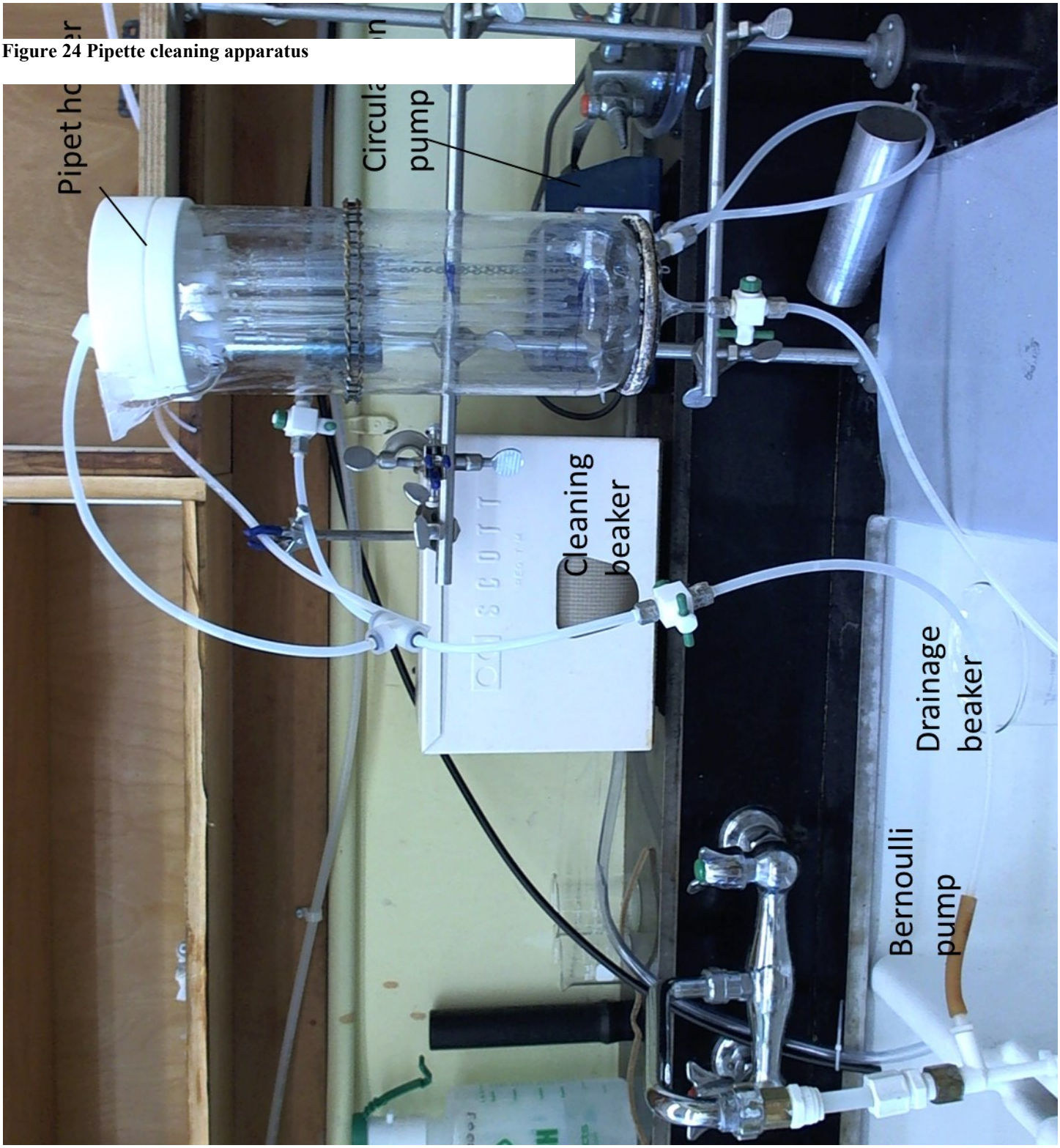

Figure 24 Pipette cleaning apparatus

A.2 Holder and bag cleaning apparatus

Some of the equipment used in cleaning both the bags and the Fricke holder are shown in figures 25 and 26.

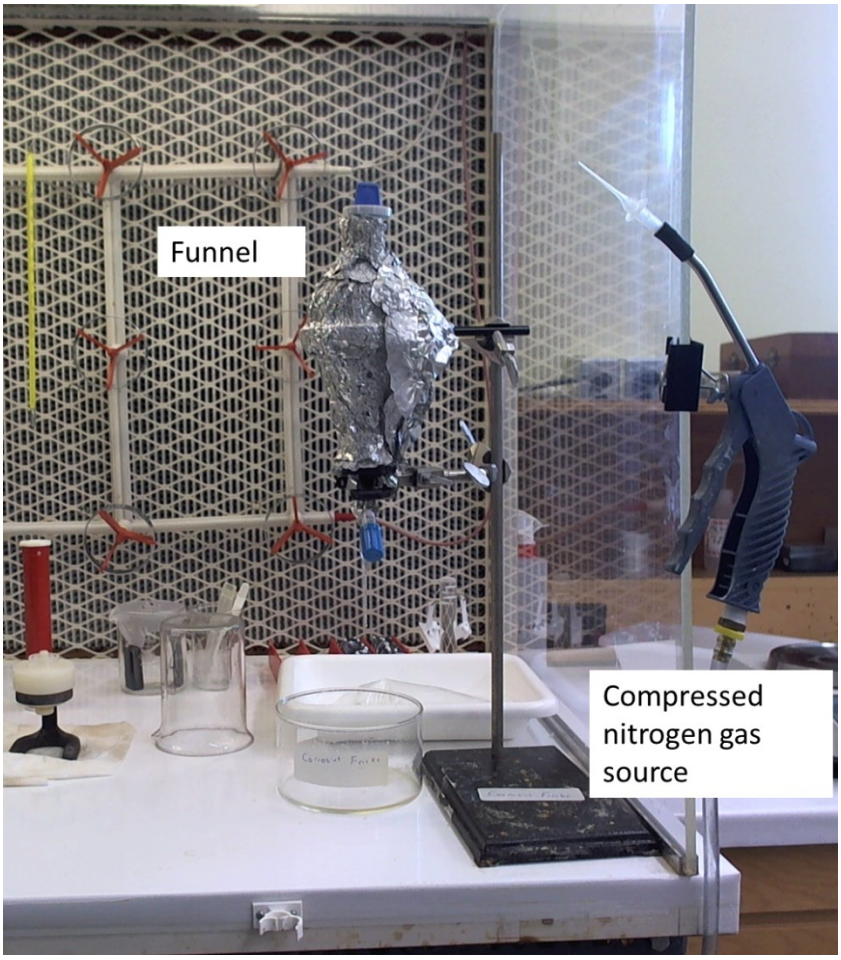

Figure 25 Fricke funnel and nitrogen source

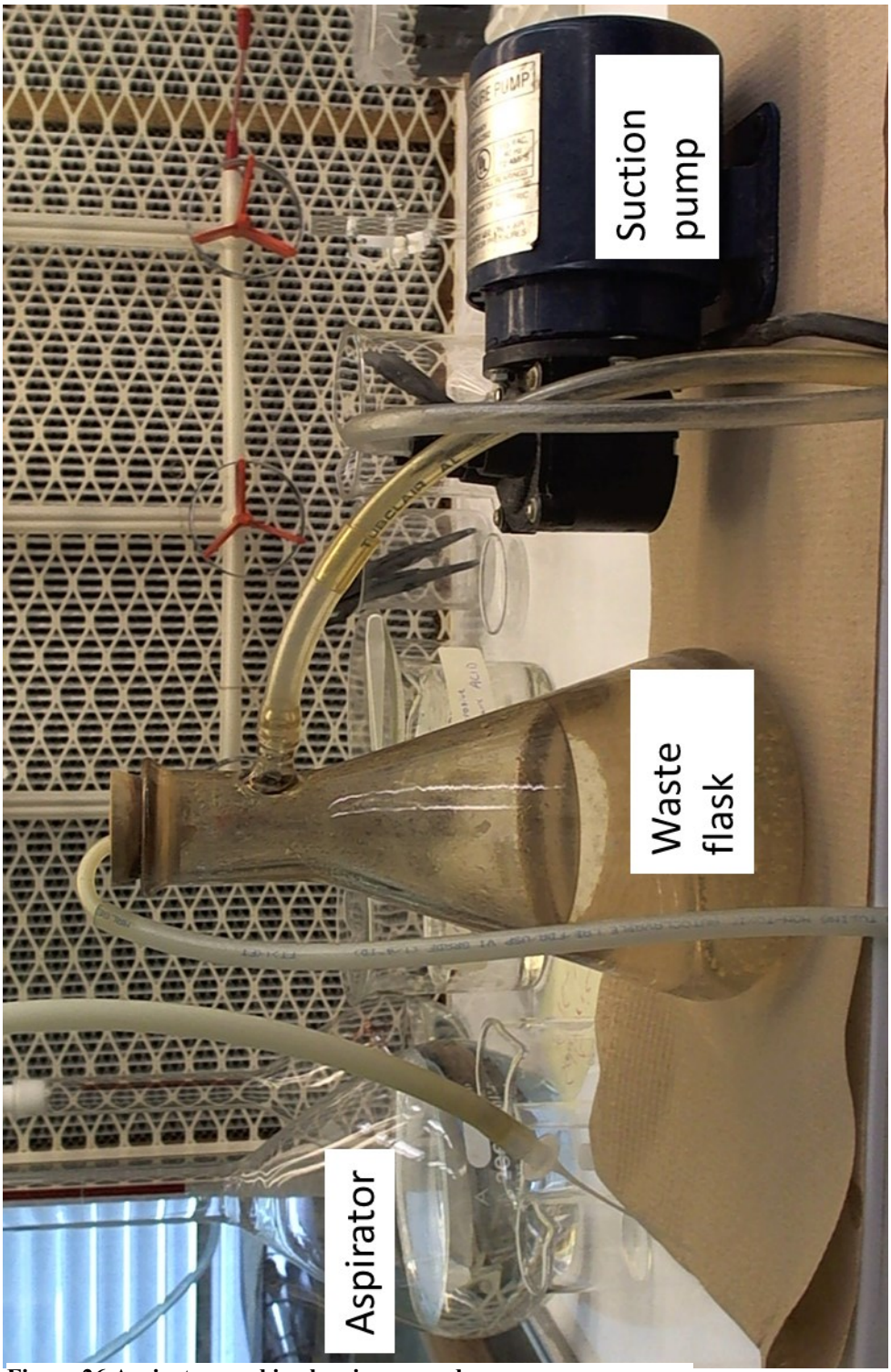

Figure 26 Aspirator used in cleaning procedures

References

Austerlitz, C., Mota, H. C., Sempau, J., Benhabib, S. M., Campos, D., Allison, R., et al. (2008). Determination of absorbed dose in water at the reference point $D(r_0,\theta_0)$ for an ^{192}Ir HDR brachytherapy source using a fricke system. *Medical Physics,* 35(12), 5360-5365.

Axtmann, R. C., and Licari, J. A. (1964). Yield of the Fricke dosimeter to 14.6 MeV neutrons. *Radiation Research,* 22(3), 511-518.

Blazy, L., Baltes, D., Bordy, J.M, Cutarella, D., Delaunay, F., Gouriou, J., Leroy, E., Ostrowsky, A., and Beaumont S. (2006). Comparison of PENELOPE Monte Carlo dose calculations with Fricke dosimeter and ionization chamber measurements in heterogeneous phantoms (18 MeV electron and 12 MV photon beams). *Phys Med* Biol 51:5951–5965.

Chauvenet, B., Baltas, D., and Delaunay, F. (1997). Comparison of graphite-to-water absorbed-dose transfers for ^{60}Co photon beams using ionometry and Fricke dosimetry. *Physics in Medicine and Biology* 42(11), 2053.

Chiu-Tsao, S., Schaart, D. R., Soares, C. G., and Nath, R. (2007). Dose calculation formalisms and consensus dosimetry parameters for intravascular brachytherapy dosimetry: Recommendations of the AAPM therapy physics committee task group no. 149. *Medical Physics,* 34(11), 4126-4157.

Carleton Laboratory for Radiotherapy Physics. (2008). *Nucletron, microSelectron-v2, HDR.* Retrieved 07/2013, 2013, from http://www.physics.carleton.ca/clrp/seed_database/Ir192_HDR/microSelectron_v2#References

Cojocaru, C., Stucki, G., McEwen, M. and Ross, C. (2010). TH-C-BRB-07: Development of a wall-less fricke dosimetry system for megavoltage photon and electron beams. *Medical physics ,* 37. (6) pp. 3454.

Davies J V and Law J 1963 Practical aspects of ferrous sulphate dosimetry *Phys. Med. Biol*. 8 91–6

Delacroix et al, Radiation Protection Dosimetry - Radionuclide and Radiation Protection Data Handbook (Kent, England: Nuclear Technology Publishing, 1998), p. 112

DeWerd, L. A., Ibbott, G. S., Meigooni, A. S., Mitch, M. G., Rivard, M. J., Stump, K. E., et al. (2011). A dosimetric uncertainty analysis for photon-emitting brachytherapy sources: Report of AAPM task group no. 138 and GEC-ESTRO. *Medical Physics,* 38(2), 782-801.

Fregene A O. (1967) Calibration of the ferrous sulphate dosimeter by ionometric and calorimetric methods for radiations of a wide range of energy *Radiat. Res*. 31 256–72

Fricke, H., and Hart, E. J. “Chemical Dosimetry” in Radiation Dosimetry, Vol. II. F. H. Attix and W. C. Roesch (eds.). New York: Academic Press, 1966.

Goetsch, S. J., Attix, F. H., Pearson, D. W., and Thomadsen, B. R. (1991). Calibration of ^{192}Ir high-dose-rate afterloading systems. *Medical Physics,* 18(3), 462-467.

International Commission on Radiation Units and Measurements. (1969). Radiation Dosimetry: x-rays and gamma rays with maximum photon energies between 0.6 and 50 MeV. ICRU Report 14 (Taylor, MD: International Commission on Radiation Units and Measurements)

International Commission on Radiation Units and Measurements. (1982). The dosimetry of pulsed radiation. ICRU Report 34 (Bethesda, MD: International Commission on Radiation Units and Measurements)

Jayson, G. G., Parsons, B. J., and Swallow, A. J. (1975). The mechanism of the fricke dosimeter. *International Journal for Radiation Physics and Chemistry, 7*(23), 363.

Klassen, N. V., K. R. Shortt, J. Seuntjens, and C. K. Ross. (1999). "Fricke dosimetry: The difference between G(Fe^{3+}) for ^{60}Co γ-rays and high-energy x-rays." *Phys Med Biol* 44:1609–1624.

Kwa W and Kornelsen R O (1990). Comparison of ferrous sulfate (Fricke) and ionization dosimetry for high-energy photon and electron beams. *Med. Phys.* 17 602–6

LaVerne, J. A., and Schuler, R. H. (1994). Track effects in water radiolysis: Yields of the fricke dosimeter for carbon ions with energies up to 1700 MeV. *The Journal of Physical Chemistry,* 98(15), 4043-4049.

Ma, C.-M., Rogers D. W. O., Shortt K. R., Ross C. K., Nahum A. E., and Bielajew A. F. (1993). "Wall-correction and absorbed-dose conversion factors for Fricke dosimetry: Monte Carlo calculations and measurements." *Med Phys* 20:283–292.

Mainegra-Hing, E., Reynaert, N., and Kawrakow, I. (2008). Novel approach for the Monte Carlo calculation of free-air chamber correction factors. *Medical Physics,* 35(8), 3650-3660.

McEwen, M. R., and Ross, C.K. (2010). Clinical dosimetry measurements in radiotherapy (AAPM 2009 summer school, CD-ROM version). *Medical Physics*, 37(5), 1027.

Nath, R., Anderson L. L., Luxton G. , A.Weaver K., Williamson J. F., Meigooni A. S. (1995). "Dosimetry of interstitial brachytherapy sources: recommendations of the AAPM Radiation Therapy Committee Task Group No. 43. American Association of Physicists in Medicine." *Med Phys* 22:209–234. Also available as AAPM Report No. 51.

Olszanski, A., Klassen N. V., Ross C. K., and Shortt K. R. (2002). "The IRS Fricke Dosimetry System. PIRS-0815. National Research Council of Canada, Ottawa, ON. http://inms-ienm.nrccnrc.gc.ca/pubs/documents/NRCC-PIRS-0815.pdf.

Perez-Calatayud, J., Ballester, F., K. Das, R., DeWerd, L. A., Ibbott, G. S., Meigooni, A. S., et al. (2012). Dose calculation for photon-emitting brachytherapy sources with average energy higher than 50 keV: Report of the AAPM and ESTRO. *Medical Physics,* 39(5), 2904-2929.

Pimblott, S. M., and LaVerne, J. A. (2002). Effects of track structure on the ion radiolysis of the Fricke dosimeter. *The Journal of Physical Chemistry A,* 106(41), 9420-9427.

Rasmussen, B. E., Davis, S. D., Schmidt, C. R., Micka, J. A., and DeWerd, L. A. (2011). Comparison of air-kerma strength determinations for HDR ^{192}Ir sources. *Medical Physics,* 38(12), 6721-6729.

Rivard, M. J., Coursey, B. M., DeWerd, L. A., Hanson, W. F., Huq, M. S., Ibbott, G. S., Mitch, M. G., Nath, R., and Williamson, J. F. (2004). "Update of AAPM Task Group No. 43 Report: A revised AAPM protocol for brachytherapy dose calculations." Med Phys 31:633–674. Also available as AAPM Report No. 84.

Sarfehnia, A., Stewart, K., and Seuntjens, J. (2007). An absorbed dose to water standard for HDR ^{192}Ir brachytherapy sources based on water calorimetry: Numerical and experimental proof-of-principle. *Medical Physics,* 34(12), 4957-4961.

Scharf, K., and Lee, R. M.. (1962). "Investigation of the spectrophotometric method ofmeasuring the ferric ion yield in the ferrous sulfate dosimeter." *Radiat Res* 16:115–124.

Selbach, H., Bambynek, M., Aubineau-Laniace, I., Gabris, F., Guerra, A. S., Toni, M. P., et al. (2012). Experimental determination of the dose rate constant for selected 125 I- and 192 ir-brachytherapy sources. *Metrologia,* 49(5), S219.

Shalek R J, Sinclair W K and Calkins J C (1962). The relative biological effectiveness of 22-MeVp x-rays, cobalt-60 gamma rays, and 200-kVcp x-rays. II. the use of the ferrous sulfate dosimeter for x-ray and gamma-ray beams. *Radiat. Res.* 16 344–51

Shortt, K. R. (1989). The temperature dependence of G(Fe3+) for the Fricke dosimeter. Phys Med Biol 34:1923–1926.

Shortt, K., Shobe, J., and Domen, S. (2000). Comparison of dosimetry calibration factors at the NRCC and the NIST. *Medical Physics,* 27(7), 1644-1654.

Stump, K. E., DeWerd, L. A., Micka, J. A., & Anderson, D. R. (2002). Calibration of new high dose rate ^{192}Ir sources. *Medical Physics,* 29(7), 1483-1488.

Taylor, R. E. P., and Rogers, D. W. O. (2008). An EGSnrc monte carlo-calculated database of TG-43 parameters. *Medical Physics,* 35(9), 4228-4241.

Weiss J, Bernstein W and Kuper J B H. (1954). Absolute yield of the ferrous sulfate oxidation reaction *J. Chem. Phys*.22 1593–6